Linköping University | Department of Electrical Engineering
Master's thesis, 30 ECTS | Automatic control
2023 | LiTH-ISY-EX–23/5591–SE

Modelling and control of the steering in an articulated forklift using rapid control prototyping

Modellering och reglering av styrningen för en midjestyrd truck med hjälp av rcp

Alexander Lilja and Filip Leijonhufvud

Supervisor : Muhammad Ahsan Razaq
Examiner : Martin Enqvist

External supervisor : Haider Khudair

LINKÖPING UNIVERSITY

Linköpings universitet
SE–581 83 Linköping
+46 13 28 10 00 , www.liu.se

Abstract

This report focuses on the steering of a Very Narrow Aisle (VNA) forklift, which undergoes frequent transitions between manual and wire guidance modes. Manual operation is employed outside narrow aisles, while wire guidance mode is utilized within them. VNA forklifts are commonly employed in environments where space optimization and productivity are of utmost importance.

The forklift's steering system operates hydraulically through the movement of two cylinders controlled by a proportional valve, which in turn is controlled by a current input. To implement the steering control, a Speedgoat target machine, a rapid control prototyping platform, is utilized. The control algorithm is developed in Simulink Real-Time and integrated with the forklift's MCU through the Speedgoat target machine, connected via a CAN bus.

The Speedgoat control strategy utilizes the distance from wire (DFW) and heading angle (HA) to generate a pivot angle request. In contrast, the current control strategy aims to minimize DFW, HA, and the pivot angle using P controllers. For the Speedgoat control strategy, the pivot angle request is compared to the current pivot angle to produce a steering command. A PD controller is applied to the heading angle for rapid stabilization of steering changes, while a PI controller is used to ensure the actual pivot angle follows the desired pivot angle. To minimize the distance from the wire, a P controller with two different settings, depending on proximity to wire locking is employed. The control strategy also incorporates bumpless transfer techniques to ensure smooth transitions between manual and wire guidance modes by gradually adjusting the impact of wire guidance and manual steering. Anti-windup measures are taken to prevent integral wind-up effects, and various PID tuning methods are explored to determine the optimal controller parameters.

A simulation model is developed to simulate the manual steering of the forklift. The manual steering implemented in Speedgoat exhibits smoother behavior compared to the current configuration, albeit with slightly longer time delays during start and stop events. When switching between manual and wire guidance modes, the Speedgoat configuration provides a smoother transition. This is attributed to the utilization of bumpless transfer techniques, which minimize abrupt valve switches and mitigate the undesired zig-zag motion.

In wire guidance mode, the Speedgoat configuration generally produces smaller steering commands. However, when the forklift is in close proximity to wire locking, the proportional gain is increased, resulting in higher steering commands. This accelerates the reduction of DFW, leading to a shorter time until the forklift is locked onto the wire. Thus, the Speedgoat controller can compete with the current controller in terms of locking time while maintaining smoother behavior during wire acquisition. However, smaller steer-commands reduce the likelihood for the forklift to acquire the wire when it is approached more aggressively.

Acknowledgments

We would like to thank our supervisor, Haider Khudair at Toyota Material Handling who has provided us with guidance, knowledge and support throughout the whole thesis. We would also like to thank Toyota Material Handling for making this master thesis possible and other employees who have assisted us throughout the thesis.

We would also like to thank examiner Martin Enqvist and supervisor Muhammad Ahsan Razaq for their help and guidance.

Contents

List of Figures

List of Tables

Nomenclature

Symbol	Description	Unit
A_1	Piston area for chamber 1	[m^2]
A_2	Piston area for chamber 2	[m]
A_c	Compensator area exposed to the pressure.	[m^2]
A_v	Valve opening area	[m^2]
C_q	Flow coefficient	[−]
F_0	Spring force, preloaded in the pressure compensation valve	[N]
F_l	External load force on piston	[N]
I_{valve}	The desired current for the valve	[A]
K_{ref}	Spring constant for the compensating valve	[N/m]
p_{comp}	Compensated pressure, after the pressure compensating valve	[Pa]
q_l	Flow for the load side of the cylinder	[m^3/s]
R_{valve}	The resistance for the valve coil	[Ω]
V_{batt}	Battery voltage	[V]
x_v	Spool displacement	[m]
x_{comp}	Pressure compensating valve displacement	[m]
θ_p	Pivot angle	[deg]
w	Valve area gradient	[m]
ρ	Fluid density	[kg/m^3]
Δp	Pressure difference over valve	[Pa]

Explanation of expressions

Dither signal: A low frequency signal which is superimposed over the PWM signal to the current in the solenoid and causes a small vibration.

Pivot angle: Angle between front and rear part of the forklift.

MCU: A main controller unit is a small computer chip that integrates the central processing unit with other components to manage and control the operations of electronic devices.

CAN: Controller Area Network is a communication protocol used in automotive and industrial applications to enable microcontrollers and devices to communicate with each other in real-time without a host computer.

RCP: Rapid Control Prototyping is the process of quickly creating a functional prototype of a control system using a combination of hardware and software tools.

PWM: Pulse Width Modulation is a technique for analog signal modulation that involves generating a square wave with a varying duty cycle to control the amount of power delivered to a load.

Accumulator: An accumulator stores hydraulic fluid under pressure to provide immediate or supplemental power to hydraulic systems when needed.

DC motor: A direct current motor (DC motor) is an electric machine that converts electrical energy into mechanical energy by utilizing the interaction between a magnetic field and an electric current flowing in a coil.

IFT: Iterative feedback tuning involves a systematic and incremental approach to optimize the controller's parameters by iteratively adjusting them based on feedback from the system's response.

Autostatus: When the operator actively requests wire guidance mode and the wire in the driving direction is detected (term used by Toyota Material Handling).

Abbreviations

MSE: Mean Square Error

NRMSE: Normalized Root Mean Square Error

PID: Proportional Integral Derivative Controller

MPC: Model Predictive Controller

DFW: Distance From Wire

HA: Heading Angle

VP: Virtual Point

VNA: Very Narrow Aisle

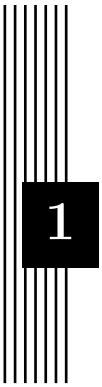

1 Introduction

1.1 Background

This analysis focuses on a Very Narrow Aisle (VNA) forklift with articulated steering. The forklift's dimensions closely match the width of the designated aisles, preventing it from executing 180-degree turns while operating within the aisles. The current configuration of the forklift includes a constant flow valve, two actuator cylinders, and an accumulator. To maintain system pressure, a pump and a DC motor are used to supply oil to the accumulator when the pressure drops below a certain threshold.

The forklift's steering is automated using wire guidance while navigating within the aisles. During aisle transitions, the operator manually controls the steering until the forklift detects the wire in the next aisle. Articulated steering is also incorporated, allowing for a reduced turning radius during these transitions. The varying driving scenarios require different performance criteria for the hydraulic system. For manual operation, the steering should be firm and enable quick turns, while accurate and smooth steering is prioritized for automated operation.

Currently, the forklift utilizes proportional valves to regulate flow and control steering. However, when operating in automated mode within the aisles, the flow volumes are small, resulting in an undesired zig-zag motion during the switch from manual to wire guidance mode. Enhancing the control system for the proportional valve could mitigate this zig-zag motion.

1.2 Related work

Several previous studies have explored the steering control of forklifts, providing valuable insights for this research. Jiang et al. [13] investigated control strategies such as linear quadratic regulator (LQR) and optimal control methods. However, recent research has focused more on autonomous forklifts, as demonstrated in [20], where a time-varying feedback control law was employed. In this thesis, the forklift under investigation is partially autonomous, featuring an automatic steering mode.

The steering system of the forklift was evaluated in a previous master's thesis by [14], which provided a comprehensive description of the mechanical and hydraulic aspects of the system. This knowledge was instrumental in understanding the system's fundamentals and developing a model. Additionally, formulas from hydraulic literature such as [8] and [17] were utilized to enhance the understanding of hydraulics.

A model for the lifting function of a forklift was designed using Simscape in a study by Bodin and Davidsson [3], where optimal control theory and model-based design were applied to develop a controller. The hydraulic system used in that forklift was similar to the one in the current forklift, motivating the adoption of a similar approach for addressing the problem. The CAD files were imported into Simscape and integrated with the forklift model.

Various control strategies, including model predictive control (MPC), feedforward from reference signal, LQR, and anti-windup techniques, are explained in works such as [6], [7], [1], [16], and [10]. These sources were consulted to determine the appropriate control strategy, considering their advantages, disadvantages, and ease of control design. Methods for achieving bumpless transfer when switching between automatic and manual control modes, as well as updating the integral part in a PI controller during mode transitions, were discussed in [6] and [4]. Additionally, [6] and [9] provided insights into different approaches for tuning PID parameters.

Hjalmarsson et al. [11] explained iterative feedback tuning (IFT) and discussed its advantages and disadvantages. One advantage is that no model is required, but a drawback is that the methodology's effectiveness is limited to specific systems, and trial and error may be necessary to set an important parameter.

In [18], the mechatronic system of a forklift is explained, including the basics of the Controller Area Network (CAN) and its application in rapid control prototyping. CAN fundamentals are also covered in [5]. Jansson and Nilsson [12] conducted a master's thesis on rapid control prototyping, developing and evaluating different control strategies (MPC and P controller) for the lifting function of a Reach Rider Electrical forklift. Despite focusing on a different function and forklift type, the thesis was relevant due to the utilization of the same communication protocol and a similar hydraulic system.Furthermore, it justified the use of rapid control prototyping, given its success in that study.

Modelling of hydraulic systems in forklifts, specifically the lifting and lowering functions, were addressed in [7] and [2]. These works also discussed control strategies such as MPC, PID, and feedforward control. Evaluation methods for assessing models, including NRMSE and MSE, were introduced in [7] and [2], serving as inspiration for model evaluation in this thesis.

1.3 Problem formulation

The current forklift employs proportional valves for steering control, which are used both in manual and automatic steering modes. However, the hydraulic flow requirements differ between manual and automatic steering, and the control system must compromise to achieve acceptable performance in both modes. This compromise can make it challenging for the steering system to effectively control the movement, particularly when transitioning between low flow in automatic mode and higher flow in manual operation. As a result, the transition between modes in the current system can lead to undesired movements.

The time taken for the mode change between manual and automatic also has implications for productivity. To activate automatic mode before entering a narrow aisle, a smooth

and timely transition is necessary. Delays or abrupt changes during the mode transition pose a risk of the forklift reaching a position inside the aisle while still in manual mode, potentially causing collisions with racks and resulting in damage. Such incidents may trigger error codes, requiring the operator to enter emergency mode and move the forklift out of the aisle. Subsequently, the forklift will need to start the process again and re-enter the aisle, leading to a loss of productivity.

To avoid these issues and enhance productivity, it is important to improve the transition between manual and automatic steering modes, allowing for a smooth and timely activation of the automatic mode before entering narrow aisles.

1.4 Purpose and goal

The goal of this thesis is to explore potential improvements for the current control system of the forklift's steering function, aiming to achieve smoother and more responsive steering. This will be accomplished by developing an algorithm based on rapid control prototyping concepts, utilizing a Speedgoat controller. The implementation of the algorithm will be carried out using Matlab/Simulink and will be simulated with a hydraulic and mechanical system in Simscape.

By implementing and evaluating the controller on the forklift, the thesis aims to assess the effectiveness of the proposed improvements in enhancing the steering performance. The use a simulation model allows for iterative testing and refinement of the control algorithm before applying it on the actual forklift. Rapid control prototyping allows for iterative testing and refinement on the actual forklift.

Through this investigation, the thesis aims to provide insights and recommendations for enhancing the control system, leading to improved steering capabilities, smoother transitions between manual and automatic modes, and ultimately increasing the productivity, driving experience and efficiency of the forklift operation.

1.5 Delimitation

In the current forklift configuration, there are two electric motors that provide movement for the wheels on each side. The steering of the forklift is influenced by the direction and speed of these motors. However, these motor effects are not considered in the analysis of the steering system for this thesis. The mass of the stand on the forklift is significant, but it is not explicitly included in the model. Instead, the weight of the stand is distributed among other parts of the forklift.

The model also disregards the friction and dynamics of the wheels, which can have an impact on the steering behavior. The focus of this thesis is solely on the hydraulic system responsible for controlling the steering, and other hydraulic systems, such as the forks, remain unchanged. The design of the steering hydraulic system itself is not modified, but rather, the modifications are made in the control system for the proportional valve.

It is important to note that the MCU controls all other functions of the forklift steering except for the currents sent to the valves. The modifications in this thesis primarily revolve around enhancing the control system for the proportional valve to improve the overall steering performance.

1.6 Outline

Chapter 1 provides an introductory overview of the problem and its context, formulating the problem statement and defining the thesis's purpose, objectives, and scope. It also discusses relevant literature and previous research related to the problem. In Chapter 2, the theoretical background and concepts related to hydraulic components, sensors, and the Speedgoat controller are presented, offering a comprehensive understanding of the fundamental principles and mechanisms underlying the hydraulic system. Chapter 3 describes the methodology employed for modeling the hydraulic system in Simscape, outlining the step-by-step process followed to create an accurate and representative model. Chapter 4 discusses the current control strategy for wire guidance in the forklift and introduces a new control strategy proposed in this thesis. A new manual control strategy is also introduced and compared with the present control strategy. Chapter 5 presents the results of model validation and control strategy evaluation, analyzing and discussing the outcomes in light of the established objectives and criteria, including strengths, limitations, and potential improvements. Finally, Chapter 6 summarizes the main findings and conclusions, discussing their implications and relevance to the field, and identifies future research areas for enhancing the steering control system.

2 Theory

This chapter focuses on providing a detailed description of the hydraulic system and its components. The hydraulic system plays a crucial role in the operation of the forklift, and understanding its components is essential for effective control.

Additionally, the chapter introduces Simscape, a Simulink-based simulation environment. Simscape enables the modeling and simulation of physical systems, including hydraulic systems. It provides a powerful tool for analyzing and testing the hydraulic system's behavior under different operating conditions.

The chapter also discusses the available sensors and their usage in deriving parameters for the wire guidance mode. Sensors play a critical role in providing feedback and measurements necessary for accurate control. By utilizing the data from these sensors, the system can determine the appropriate actions and make informed decisions during wire guidance mode.

Lastly, the chapter includes an overview of the Speedgoat system and its connection with the forklift. The Speedgoat system serves as an interface between the forklift and the control algorithms, enabling real-time control and communication. Understanding the connection and integration of the Speedgoat system with the forklift is important for ensuring efficient and reliable control of the forklift's operations.

2.1 Hydraulic System

The hydraulic scheme shown in Fig. 2.1 represents the hydraulic system used in the forklift, sourced from Toyota Material Handling. The system utilizes single-acting cylinders controlled by a proportional valve.

The operation of the cylinders involves the proportional valve supplying flow to the high-pressure side of the cylinder, while the low-pressure side is connected to a tank. This arrangement allows for controlled movement of the cylinders. The proportional valve regulates the flow of pressurized oil, enabling precise control over the steering angle of the forklift.

To ensure an adequate supply of pressurized oil, an accumulator is incorporated into the

system. The accumulator is charged by a hydraulic pump, maintaining a sufficient pressure level. The pressure difference created by the accumulator drives the flow through the valve, facilitating the movement of the cylinders and, consequently, the change in the forklift's steering angle.

For safety purposes, the hydraulic system includes multiple pressure relief valves. These valves are designed to prevent the pressure levels from exceeding a predetermined threshold. By limiting the maximum pressure, the relief valves ensure the system operates within safe limits, mitigating the risk of damage or failure.

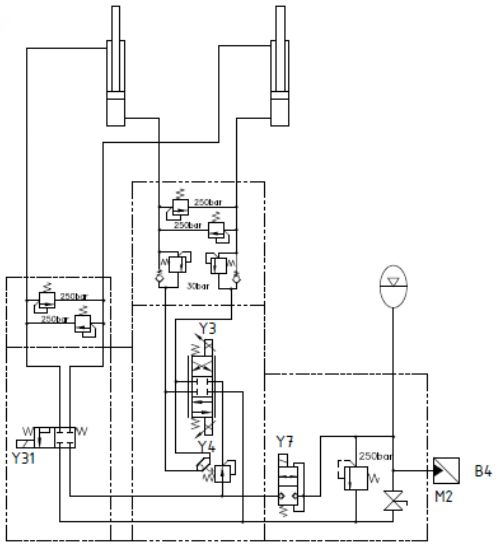

Figure 2.1: *Hydraulic scheme of the forklift.*

2.1.1 Proportional valve

The proportional valve plays a crucial role in controlling the flow of oil to the hydraulic actuators. The valve's movement, which determines the flow rate, is controlled by a current input. When a current is applied to the solenoids, it generates a force that causes the spool to move either to the right or to the left, depending on the signal. This movement of the spool controls the flow of oil from the supply port to either port A or port B, thereby controlling the movement of the hydraulic cylinders.

However, the relationship between the applied current and the resulting flow rate is non-linear. This nonlinearity is mainly due to two factors: the dead zone and the hysteresis effect. The dead zone refers to a range of currents where the valve does not respond or exhibit any significant movement. Similarly, the hysteresis effect causes the opening current to differ from the closing current, resulting in a different response depending on the direction of the current change.

To improve the linearity and response time of the valve, a dither signal is employed. The dither signal introduces small oscillations in the valve's movement, increasing linearity by reducing the stick-slip effect. This effect occurs when static friction is present, and the valve spool tends to stick rather than move smoothly. By introducing the dither signal, the static friction is overcome, leading to smoother and more precise control of the valve's displacement.

In a simple system with a proportional valve, as shown in Fig.2.2, the valve displacement x_v

determines the direction of the flow and the pressurized cylinder chamber. The opening area of the valve depends on the valve displacement and restricts the flow. Since the opening area is variable, the flow over the proportional valve can be described by the flow equation for a variable orifice [8] described as

$$q_l = C_q A_v \sqrt{\frac{2}{\rho}\Delta p}, \quad A_v = w x_v \tag{2.1}$$

where Δp is the pressure drop over the proportional valve, w is the area gradient, C_q is the flow constant and ρ is the density of the fluid. The area gradient, the flow constant and the density are constant which means that the flow over the valve depends on the spool displacement and the pressure drop over the valve. The square root of the pressure difference leads to a nonlinear system which is not ideal from a control perspective. This is solved with a constant flow valve.

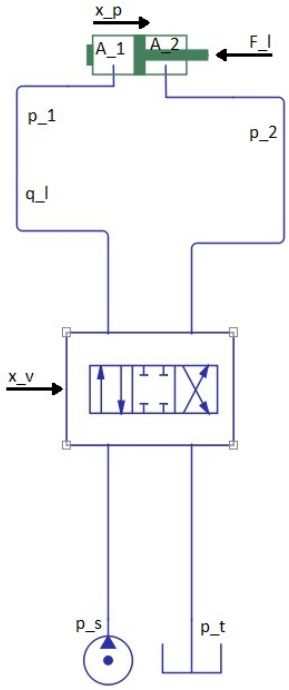

Figure 2.2: *Schematic for a proportional valve*

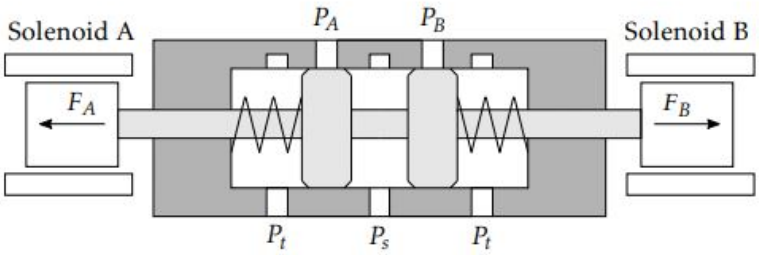

Figure 2.3: *Proportional valve showing how solenoid forces affect the spool position. This figure is taken from [3]*

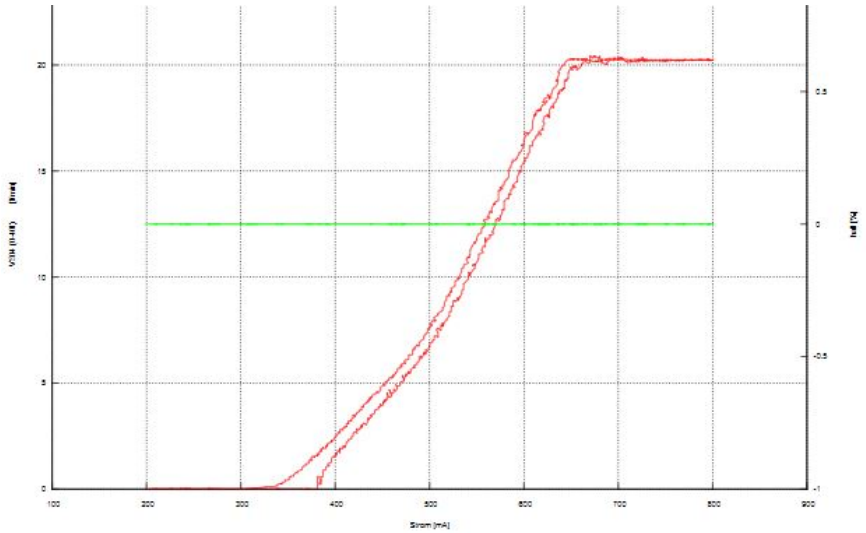

Figure 2.4: *How the input current on the the solenoids affect the flow through the valve with hysteresis shown. The input current is displayed on the x-axis, the flow is shown on the y-axis. The red image shows how the flow depends on the input current. This figure is provided by Toyota Material Handling.*

2.1.2 Constant flow valve

The combination of a pressure compensating valve and a directional valve connected in sequence is called a constant flow valve (Fig. 2.5). The principle of a pressure compensating valve is to keep the pressure difference over the proportional valve constant.

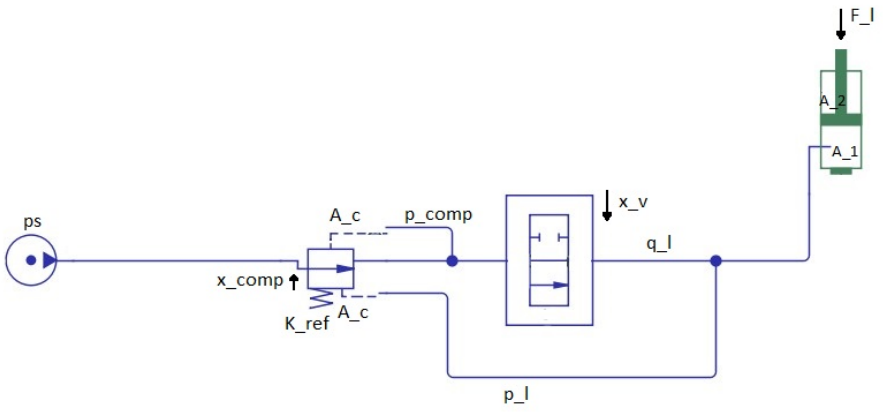

Figure 2.5: *Schematic for a constant flow valve*

Using force equilibrium for the pressure compensating valve leads to the equation 2.2 [17].

$$A_c p_l - A_c p_{comp} + (F_0 - K_{ref} x_{comp}) = 0 \Leftrightarrow p_l - p_{comp} = \frac{F_0 - x_{comp} K_{ref}}{A_c} \tag{2.2}$$

Equation (2.2) together with (2.1) gives.

$$q_l = C_q A_v \sqrt{\frac{2}{\rho}\left(\frac{F_0 - x_{comp} K_{ref}}{A_c}\right)} \tag{2.3}$$

The flow is now independent of the pressure drop over the valve (i.e. the flow has a linear dependency of the opening area). This system is much easier to work with from a control perspective. The preload force F_0 and the spring constant K_{ref} can also change the flow but are design parameters which are kept constant during operation to maintain a linear system.

2.2 Simscape modelling

Simulink Simscape is an advanced simulation tool integrated into the Simulink environment, designed to facilitate the modeling and simulation of dynamic physical systems. It enables users to construct models by utilizing components from various domains, including mechanical, electrical, and hydraulic systems. Simscape provides a comprehensive library of pre-built components, empowering users to create complex models and systems with ease.

The tool offers a range of features to enhance the simulation process. Users can select appropriate solvers to ensure accurate and efficient simulations, and they have the flexibility to fine-tune model parameters for optimal performance using the parameter tuning capabilities. Simscape also provides robust data visualization tools, enabling users to analyze and interpret simulation results effectively.

When working with Simscape, it is important to consider the potential complexity of the resulting model. While constructing a basic model may seem straightforward, each block in the model encapsulates underlying equations, which can contribute to increased complexity. In some cases, a more advanced model may be necessary to accurately resemble the real-world system. However, it is essential to note that introducing more components also introduces additional sources of error that should be taken into account during the modeling process.

2.3 Sensors

The forklift is equipped with several sensors, and among them, the ones relevant for steering control are the sensors for pivot angle, wire distance, magnetic wire voltage, and battery voltage. Notably, the voltage sensors responsible for detecting the wire voltage are positioned both at the front and rear ends of the forklift. Specifically, voltage sensors are placed on the right, center, and left sides at both the front and back of the forklift.

2.4 Calculation of important signals

An interpretation of the sensor signals is provided in Fig. 2.6. The distance from wire (DFW) is determined by the the voltage levels of the antennas. The heading angle is calculated according to

$$HA = \arcsin\left(\frac{DFW_{load} - DFW_{tractor}}{d_{antennas}}\right) \tag{2.4}$$

where $d_{antennas}$ is the distance between the load antenna and the tractor antenna given in millimeters. Assuming small heading angles during wire guidance, (2.4) can be approximated as

$$HA \approx \frac{DFW_{load} - DFW_{tractor}}{d_{antennas}} \tag{2.5}$$

When both the load and tractor antennas are detected, the controller utilizes a parameter called the virtual point distance (DFW_{VP}). This distance represents the distance from the

wire, either 1000 mm in front or behind the forklift, depending on its driving direction. An illustration of DFW_{VP} is provided in Fig. 2.6, and the equations necessary for its calculation are given in (2.6) and (2.7). The value of DFW_{VP} depends on both DFW_{load} and $DFW_{tractor}$.

By using DFW_{VP}, the controller considers both DFW_{load} and $DFW_{tractor}$ as a single signal, resulting in smoother behavior compared to using only DFW. The selection of whether to use DFW_{load} or $DFW_{tractor}$ is based on the direction of the forklift's drive speed. If the drive speed is negative, indicating that the forklift is reversing, the value of $DFW_{tractor}$ is used. Conversely, if the drive speed is positive, indicating forward motion, the value of DFW_{load} is used.

$$DFW_{VP,load} = DFW_{load} + HA * 1000 \tag{2.6}$$

$$DFW_{VP,tractor} = DFW_{tractor} - HA * 1000 \tag{2.7}$$

For the continuation of this report, the distance from wire utilized by the controller will be referred to as DFW.

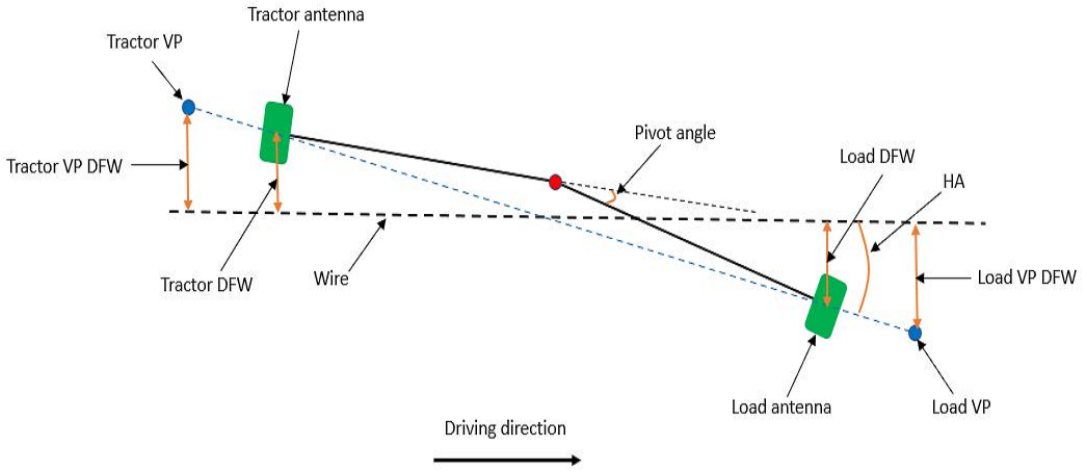

Figure 2.6: *An illustration over the forklift. The distances and angles are defined in such way that the DFW_{load} and HA are defined as positive in the figure and $DFW_{tractor}$ and pivot angle are defined as negative in the figure.*

2.5 Speedgoat rapid control prototyping

The rapid control prototyping process involves the use of a Speedgoat real-time target machine as the hardware component, while the controller is developed using Simulink. Unlike the traditional approach of using a main controller unit (MCU), the Speedgoat machine is responsible for calculating the currents required to operate the valves, which control the movement of the cylinders and consequently affect the steering of the forklift [12]. All other operations, except for the valve control, are handled exclusively by the MCU. The system architecture is illustrated in Fig.2.7.

For communication purposes, the Controller Area Network (CAN) bus protocol is employed. CAN facilitates communication between nodes using two wires, namely CAN low and CAN high. The utilization of CAN offers several advantages, including robustness, efficiency, low cost, and simplicity [5]. Data transmitted over the CAN bus can be logged and analyzed using tools such as Canalyzer.

During manual driving mode, the controller receives signals such as battery voltage, pivot angle, and steering wheel input through the CAN from the MCU. These signals are transmitted to the Speedgoat target machine for processing. On the other hand, in wire guidance driving mode, the controller receives signals including pivot angle, battery voltage, and auto-status through CAN from the MCU, which are then forwarded to the target machine.

Additionally, the MCU receives voltage readings from the various antennas, calculates wire distance and heading angle based on these voltages, and transmits the calculated values to the target machine via CAN. The target machine imports these values into the controller. The controller generates pulse-width modulation (PWM) signals as outputs, which are sent back to the MCU through CAN. The MCU utilizes these PWM signals to control the movements of the cylinders in the forklift [18].

To provide a visual representation of the system setup, Fig.4.2 illustrates the Simulink scheme for manual mode, while Fig.4.4 showcases the setup for wire guidance mode.

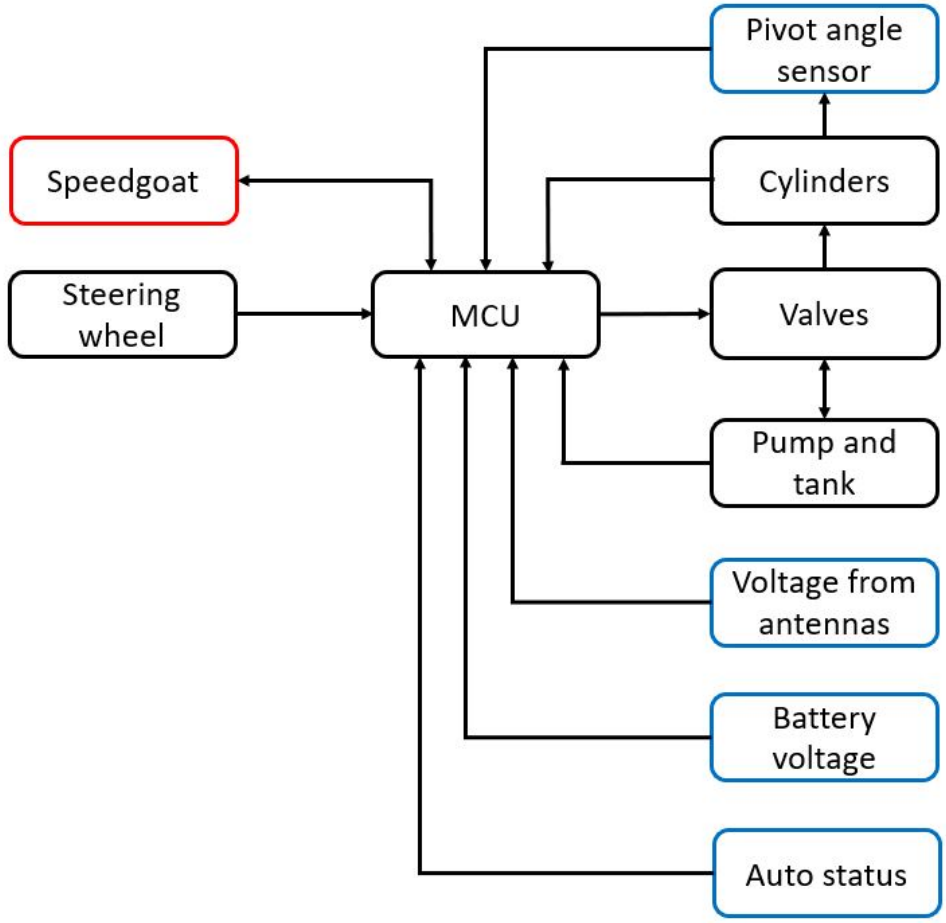

Figure 2.7: *A schematic illustration of the most relevant parts and signals of the system. The blue boxes represent sensors.*

3 Model

In this chapter, the modeling of the forklift system is presented, encompassing both the mechanical and hydraulic systems. Extensive analysis and examination of the system's fundamental properties have been conducted to ensure the development of a reliable and accurate model. This model serves as a crucial tool in the development of control algorithms, allowing for the creation of a highly precise control system that can be tested prior to implementation on the physical machine. The comprehensive model, depicted in Fig. 3.1, is constructed using Simscape.

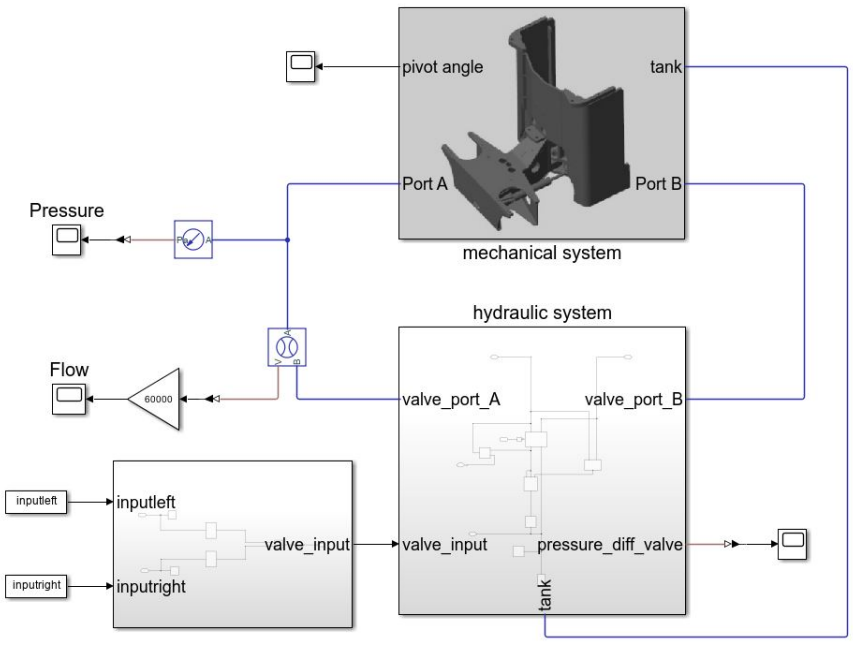

Figure 3.1: *The complete Simscape model of the system.*

3.1 Hydraulic system

The hydraulic system of the forklift has been modeled using Simscape Fluids, utilizing various blocks and components specifically designed for hydraulic systems. The hydraulic model, shown in Fig. 3.2, is based on the hydraulic steering system scheme depicted in Fig. 2.1. However, certain simplifications and approximations have been made to streamline the modeling process and determine the values of adjustable parameters.

To capture the behavior of the proportional valve, a lookup table was created using the valve characteristics presented in Fig. 2.4. For simplicity, it was assumed that the valve characteristics for both opening and closing were the same. The stroke lengths of the cylinders were determined from CAD drawings, and negligible leakage and small friction were assumed in the cylinders.

In the actual forklift, the pressure source is an accumulator with a variable pressure range of 130-210 bar. However, in the model, a constant pressure source with a pressure of 170 bar is used. To achieve a linear flow response, a constant flow valve is implemented in the model. This is accomplished by combining a shuttle valve and a pressure compensating valve. The shuttle valve allows fluid to flow through it and switches the flow between two paths based on the path with the highest pressure. The pressure compensating valve should compensate for the load pressure and the shuttle valve makes sure that it always compensates for the load pressure.

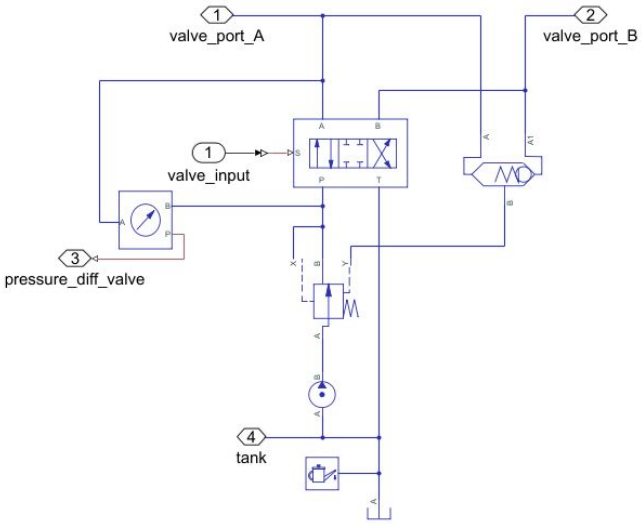

Figure 3.2: *The Simscape model of the hydraulic system.*

3.2 Mechanical system

The mechanical system of the forklift is represented in the model by the rear part, front part, and two cylinders, as shown in Fig. 3.3. CAD models of these parts have been imported into Simscape and connected according to the assembly shown in Fig. 3.4.

The front and rear parts are interconnected, as well as connected to the cylinders and the world frame. The bottom part of each cylinder is attached to the rear part, while the top part of the piston is attached to the front part. Joints are used between the parts to define their relative movement. These joints determine how the parts can move in relation to each other, allowing for the simulation of realistic mechanical behavior.

The world frame serves as a reference point for the model, and it is connected to the rotation point of the forklift where rotation is only permitted around a single axis. This constraint models the steering mechanism of the forklift.

To accurately represent the weight distribution of the forklift, the weights of the front and rear parts were manually assigned based on the weight distribution of the actual components. While the model does not include all the components of the complete forklift, it is essential to incorporate the correct weight distribution for evaluating the steering behavior. The weight of the cylinders is automatically computed from the CAD files.

The connections between the cylinders are established using joints that allow movement along a single axis.

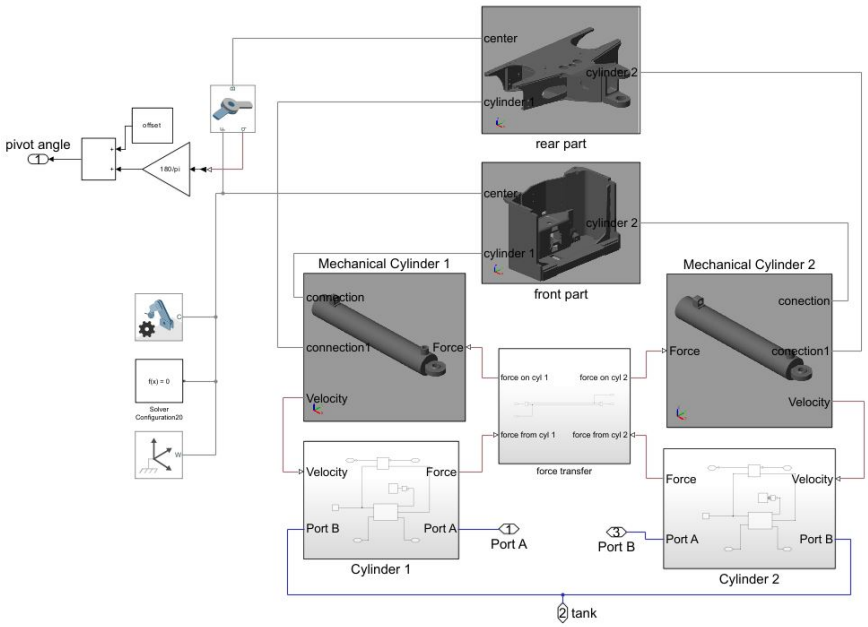

Figure 3.3: *The Simscape model of the mechanical system.*

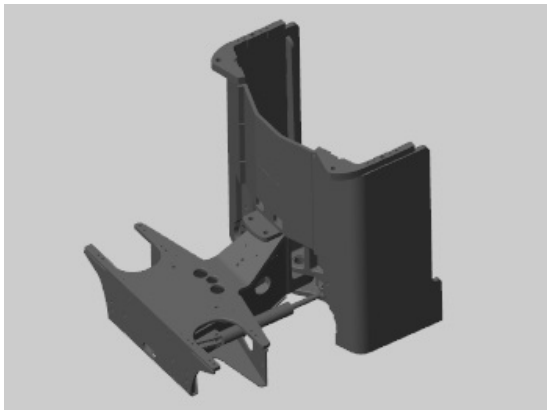

Figure 3.4: *An image of what the final assembly looks like while simulating when the parts are connected.*

3.3 Model validation

Various methods can be employed to validate the accuracy of a model. One commonly used method is the normalized root-mean-square-error (NRMSE), which is discussed in [7]. The NRMSE provides an estimate of how well the model aligns with the measured data.

$$NRMSE = \frac{1}{N} \sum_{i=1}^{N} \left(\frac{\hat{\theta}_p - \theta_p}{\theta_p} \right)^2 \tag{3.1}$$

outlines the calculation process for the normalized root-mean-square-error where N is the number of sampling-points and $\hat{\theta}_p$ is the estimated pivot angle. The model fit in percentage can be calculated as

$$model\ fit = 100(1 - NRMSE) \tag{3.2}$$

Another validation approach, employed in [2], is the mean square error (MSE), which by itself does not provide meaningful insights. In contrast, the NRMSE yields values ranging from 0 to 1, where 0 represents a perfect fit and 1 indicates a fit equivalent to a straight line along the x-axis. As the model under consideration is not being compared to another model, the NRMSE is used to validate its accuracy within this report.

4 Control

The objective of the control design is to reduce the zig-zag motion when the forklift transitions from manual to wire guidance mode. Additionally, factors such as comfort and quickness are considered for the manual and wire guidance modes. In this chapter, the present control strategy, the Speedgoat control strategy, and the manual steering are described.

4.1 Manual control strategy

The control strategy for manual steering is a proportional controller without feedback, creating an open loop system. However, considering the driver involvement and the driver's response to the output signal, the system can be seen as a closed-loop system. The controller takes the steering speed command from the steering wheel as input and generates the desired current for each steering valve as output. The maximum input from the steering wheel is 1800 units, but inputs exceeding 1040 units result in the maximum current (as shown in Fig. 4.1). This enables easy attainment of a fully open valve, avoiding the need for excessively fast steering wheel movements that may inconvenience the driver.

The proportional gain of the controller is variable, see Fig.4.1. 50% of maximum steering wheel input is 520 units, which happens after 35 seconds in Fig. 4.1. The current from the controller at this time has reached 70% of the current range (the maximum current subtracted by the opening current). The variable gain can be modified by changing a parameter, which is set to 70% in this configuration. If the variable gain parameter is set to 50%, the relation between valve opening and current is linear (in between the saturation's) and if the parameter is below 50%, the steering is less sensitive. On contrary, if this parameter has a value larger than 50%, the steering is more sensitive. The current when a steering signal is applied varies between the opening current and the maximum current, which is equivalent to a fully open valve (Fig. 4.1). The specific opening and maximum current values vary between forklifts, necessitating recalibration when a new forklift is used. The maximum current is slightly limited when the pivot angle exceeds 40 degrees and further limited when it surpasses 50 degrees, approaching the maximum pivot angle of 52 degrees. This implementation prevents abrupt stops at the end positions.

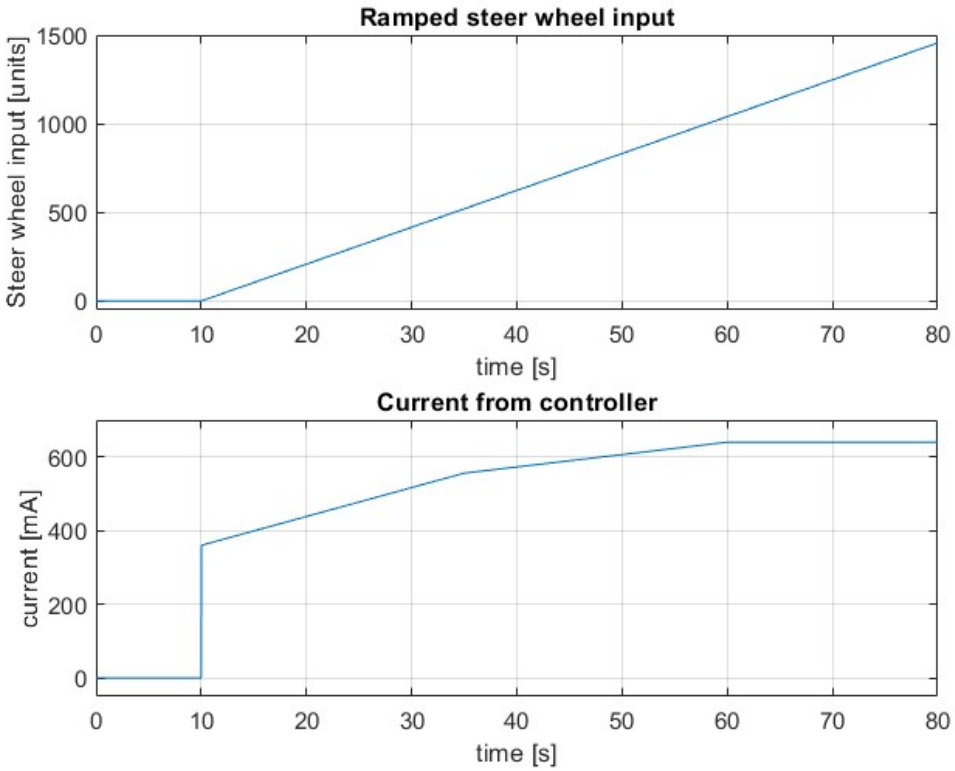

Figure 4.1: *A visualization of how the current from the controller depends on the input from the steering wheel. The principle of the variable gain is visualized alongside the opening and maximal current.*

The control strategy was initially developed and tested on a simulation model. Once satisfactory behavior was achieved in the simulation, the controller was implemented on hardware. However, during the hardware implementation, it became evident that the controller's response was excessively quick, resulting in jerky behavior. To address this issue, a rate limiter was introduced to restrict the derivative of the output currents, and a low-pass filter was incorporated to attenuate higher frequencies. The extent of derivative limitation and signal attenuation is parameterized and adjustable. A smaller value for the rate limiter produces a smoother and slower steering response, while a larger value yields a faster but bumpier steering behavior. Similarly, increasing the number of attenuated signals results in a smoother and slower steering response. These parameters are tuned to strike a balance between smoothness and response time. Achieving this balance can be challenging as preferences for steering feel vary significantly among individuals. However, some objective factors such as responsiveness and comfort (lack of bumpiness) are considered. The Simulink scheme used for running the manual controller on hardware is depicted in Fig. 4.2.

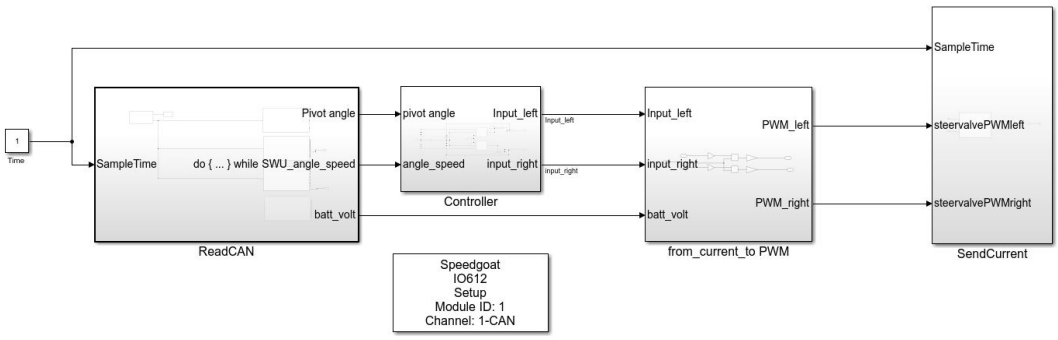

Figure 4.2: *The Simulink scheme used while running the manual controller on hardware.*

The input to the valve on the hardware is a PWM signal. The percentage of the battery voltage that should be used can be calculated as

$$pct_V = \frac{100 I_{valve} R_{valve}}{V_{batt}} \tag{4.1}$$

where I_{valve} is the desired current for the valve (this is what the controller calculates). R_{valve} is the resistance for the valve coil which is 19 Ω and V_{batt} is the voltage from the battery which can vary between 30 V and 48 V. The battery voltage is provided by a sensor. The PWM signal sent to the valve can be described as

$$PWM = 10.23 pct_V \tag{4.2}$$

where the conversion rate is 10,23.

4.2 Control strategies

When selecting a control strategy, several factors must be considered, including the availability of a model, computational capacity, performance expectations and system complexity.

A PID controller is a feedback control system that adjusts an output variable based on the error, which is the difference between the desired reference value and the actual output. The controller minimizes this error by employing proportional, integral, and derivative actions, thus enhancing the overall response of the control system.

On the other hand, a Linear Quadratic (LQ) controller is an optimal control strategy that utilizes a mathematical model of a system to minimize a quadratic cost function. This is accomplished by adjusting the control inputs of the system. An LQ controller relies on a linear system model. If the system is nonlinear, the LQ controller can still operate by linearizing the system around an operating point [10].

Model Predictive Control (MPC) involves predicting the future behavior of a system using a mathematical model to optimize the control inputs over a finite time horizon. MPC necessitates a system model and significant computational power since it solves the optimization problem at each time step.

Feedforward control, which involves using a reference signal, can be advantageous if the system is well-known. In such cases, the user can determine the transfer function between the input and output signals to a large extent. However, if the system is not well-known, this strategy is less effective.

The absence of an accurate model for wire guidance mode excluded model-based control strategies such as LQ-control, MPC and feedforward control from reference signal.

4.3 Present control strategy for wire guidance

The present control strategy for wire guidance incorporates three P controllers for the pivot angle, HA, and DFW. These controllers calculate the steering command, which determines the input signal to the valves. The steering commands for the HA and pivot angle are influenced by the forklift's travel speed, with higher travel speeds resulting in higher steering commands. Additionally, the forklift turns more when it is farther away from the wire.

To ensure safe wire acquisition, the steering command is limited to 500 units (compared to the maximum of 1800 units for manual steering). Once the forklift is locked onto the wire, the steering command limit is further reduced to 100 units.

The current controller is implemented using C code, providing a programming language suitable for efficient execution on the hardware.

The control strategy aims to minimize three key properties: DFW, HA, and the pivot angle. However, there is a conflict between minimizing the pivot angle, which restricts the forklift's turning, and minimizing DFW and HA. This conflict arises because smaller pivot angles limit the forklift's ability to get closer to the wire or adjust the HA effectively.

To address this challenge, the current control strategy takes into account all three parameters (HA, DFW, and pivot angle) when determining the steering command. As a result, the pivot angle will not necessarily be minimized if HA and DFW are large since the steering command directly influences the pivot angle. This control structure must find a compromise that allows for efficient maneuvering while still minimizing DFW, HA, and pivot angle as much as possible.

The control structure, depicting how HA, DFW, and the pivot angle are considered in determining the steering command, is illustrated in Fig. 4.3.

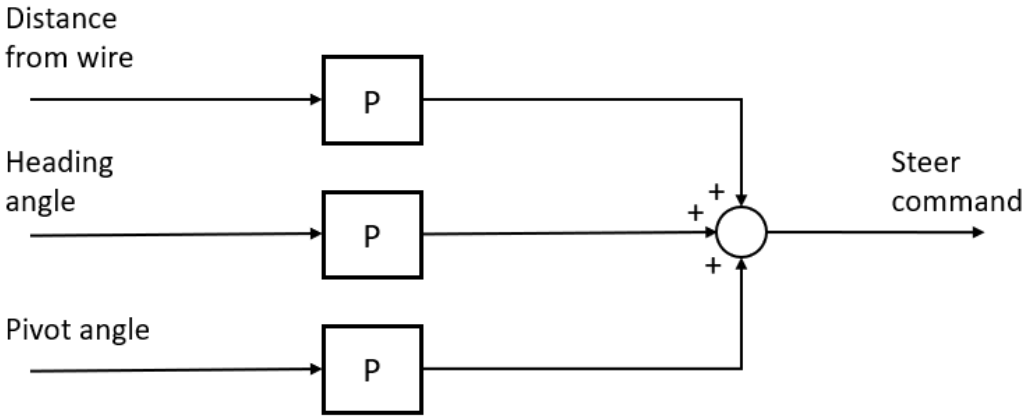

Figure 4.3: *The control structure for the present wire guidance controller.*

4.4 Proposed control strategy for wire guidance

The control strategy implemented on the Speedgoat is explained in this section. The Simulink scheme used while running the wire guidance controller on hardware can be seen in Fig.4.4. This Simulink scheme implements both manual and wire guidance modes.

4.4.1 Requirements to acquire wire

In order for the forklift to acquire the wire and enter wire guidance mode, several conditions and actions need to be met.

Firstly, the driver needs to actively press a button to initiate the wire acquisition process. Additionally, for forward driving, the wire needs to be detected by the load antenna, while for reverse driving, it should be detected by the tractor antenna. Only when the wire is detected and the auto-request feature is enabled, the auto-status becomes active.

Furthermore, the forklift cannot acquire the wire if the attack angle between the forklift and the wire is too large. This ensures that the alignment between the forklift and the wire is suitable for wire guidance.

To be locked on the wire, certain limits must be met for the pivot angle, HA, and DFW. These limits ensure that the forklift maintains stable and reliable wire guidance. Once the forklift is successfully locked on the wire, there are additional limits on the pivot angle, HA, and DFW to maintain the full-speed locking condition. If any of these limits are exceeded, the forklift will slow down until the values return within the prescribed boundaries for full-speed locking.

These conditions and limits ensure proper wire acquisition, reliable wire guidance, and safe operation of the forklift in wire-guided mode.

4.4.2 Control structure for the Speedgoat

In the wire guidance mode, a control structure consisting of a P controller, a PD controller, and a PI controller is utilized to manage the DFW, the HA, and the pivot angle.

A P controller is employed to minimize the distance from the wire, while a PD controller is employed to minimize the heading angle. The sum of the outputs of these controllers generates a pivot angle request, which is then compared to the current pivot angle. The difference between the pivot angle request and the current pivot angle is used to calculate the steering command.

To ensure that the actual pivot angle follows the desired pivot angle, a PI controller is utilized on the control error. The output of the PI controller is used to calculate the steer command. The integral part of the PI controller helps eliminate any constant control error and ensures that the forklift becomes completely upright after a settling time. The derivative part of the controller stabilizes rapid changes in steering angle while the forklift is in the process of acquiring the wire [9].

To mitigate the effects of high-frequency noise and disturbances in the input signal, a low-pass filter is applied to the PD controller. This filter helps attenuate high-frequency components, ensuring smoother control signals.

The control structure, incorporating these controllers and filters, is shown in Fig.4.5. In contrast to the present control strategy that simultaneously minimizes the HA, DFW, and

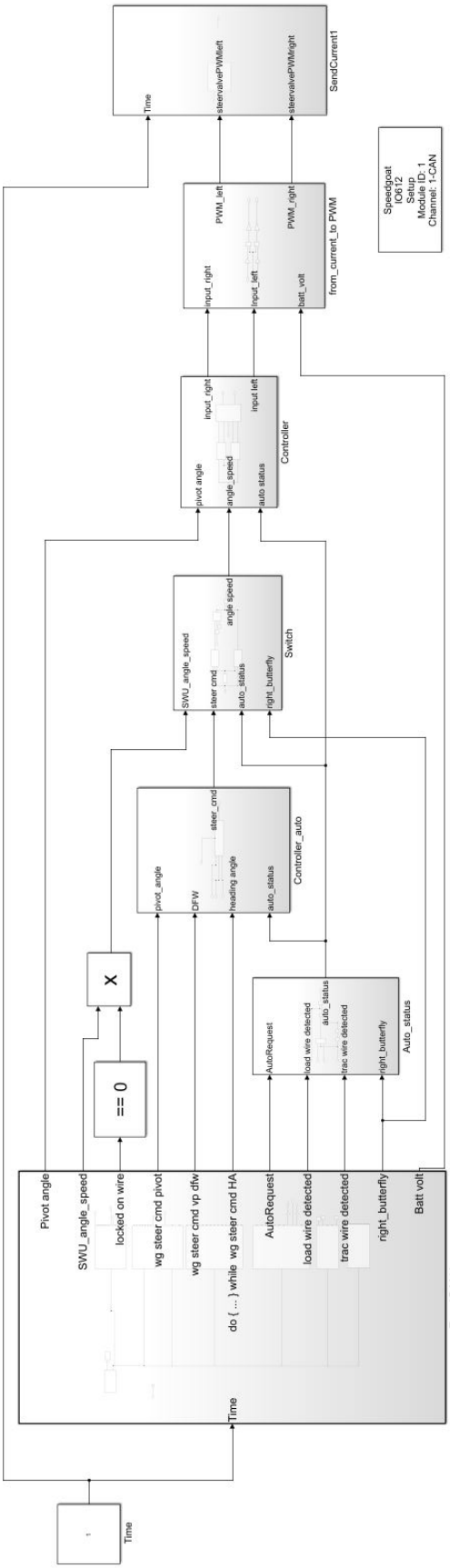

Figure 4.4: *The Simulink scheme used while running the wire guidance controller on hardware.*

pivot angle, the Speedgoat control strategy takes a different approach. It focuses on minimizing HA and DFW, while adapting the pivot angle accordingly. This strategy recognizes that all three signals are interdependent, and conflicts can arise when attempting to minimize all of them simultaneously.

By prioritizing the minimization of HA and DFW, the Speedgoat control strategy achieves greater efficiency in situations where the signals depend on each other. However, the pivot angle must be minimized for the forklift to be able to drive on the wire but it is only important that the pivot angle is small when the forklift is close to being locked onto the wire or already locked on.

When DFW and HA values are small, indicating proximity to the wire and readiness to be locked on, the corresponding pivot angle request is also small. This active minimization of the pivot angle during these critical situations ensures effective wire acquisition and alignment. By adapting the pivot angle according to the state of DFW and HA, the control strategy optimizes the overall performance and safety of the wire-guided forklift. In the Speedgoat control strategy, this is effectively implemented.

The proportional part of the P controller is adjusted dynamically based on the values of DFW and HA, particularly when they are small and close to the conditions required to lock on the wire. This modification is implemented to increase the significance of being in close proximity to the wire, as indicated by a small DFW value.

During this stage, the HA is relatively small, indicating that the forklift is approaching alignment with the wire. In this scenario, the prioritization between maintaining an upright forklift and being close to the wire is modified to expedite the process of locking on. By increasing the proportional gain of the P-controller, the control strategy places greater importance on achieving close proximity to the wire and facilitates faster wire acquisition.

Without this adjustment in the proportional gain, there is an increased risk of the forklift ending up outside the full speed locking conditions even when it has successfully locked on to the wire. By dynamically modifying the proportional gain based on the DFW and HA values, the control strategy mitigates this risk and ensures that the forklift remains within the desired operating conditions for efficient and safe wire-guided operation.

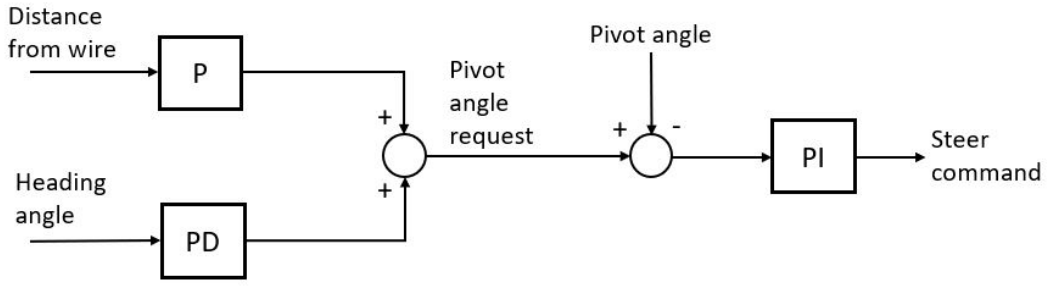

Figure 4.5: *The control structure for wire guidance mode.*

4.4.3 The interplay between the manual and the wire guidance controller

In the wire guidance mode, the steering-command calculated by the wire guidance controller is used as a replacement for the steering wheel input to the manual controller. However, there are some differences in the calculations of the currents between the wire guidance mode and manual mode, specifically aimed at achieving a smoother behavior during wire guidance.

Firstly, the steering-command in wire guidance mode is not filtered by a low-pass filter, unlike in manual mode. This omission allows for more immediate response to changes in the control signals, enhancing the agility of the forklift during wire guidance.

Additionally, the rate limiter, which limits the rate of change of the signals, is not as restrictive in wire guidance mode compared to manual mode. This modification allows for relatively faster adjustments in the control signals during wire guidance, contributing to quicker maneuvering.

Moreover, the variable gain parameter, initially set to 70% in the manual controller, is reduced to 10% for wire guidance mode. This adjustment is implemented to create a smoother behavior, particularly considering that the signals involved in wire guidance mode are typically smaller in magnitude compared to manual mode.

In situations where there is no speed-request from the driver, it is not desired for the forklift to actively try to acquire the wire, even if the auto-request is active. Consequently, in such cases, there is no steering-command generated from the wire guidance mode.

This design decision ensures that the forklift does not initiate wire acquisition when the driver does not intend to engage in wire-guided operation. By considering the absence of a speed-request as an indication that wire guidance is not currently desired, the control system effectively prevents any unintended wire acquisition attempts.

This approach promotes safety and allows the driver to maintain full control over the forklift's operational mode. Wire guidance mode is only engaged when there is an explicit speed-request from the driver, ensuring that the forklift operates in the intended mode based on the driver's intentions and commands.

Overall, these changes in the wire guidance mode's control calculations are specifically tailored to accommodate smaller signals and promote a smoother operational behavior, ensuring precise and controlled movements during wire-guided forklift operations.

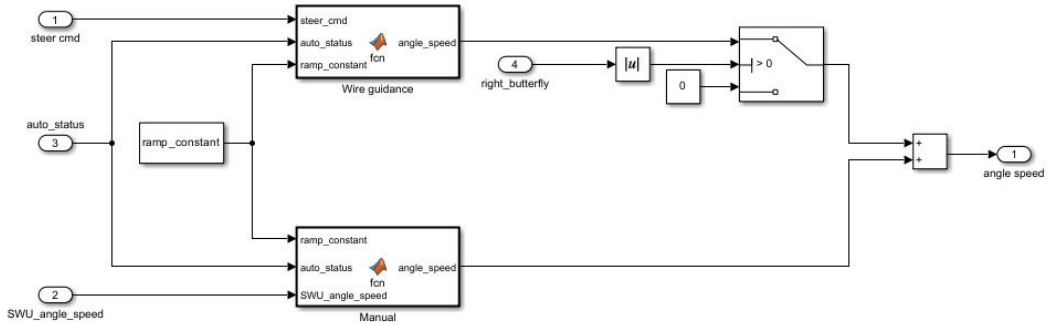

Figure 4.6: *The interplay between the manual and the wire guidance controller. The MATLAB functions here are bumpless transfer functions, see Appendix B.*

4.4.4 Bumpless transfer

Bumpless transfer is a technique employed to minimize disturbances during transitions between different controllers, particularly when they operate in distinct modes or with varying parameters. In the context of this thesis, bumpless transfer is used to ensure a smooth and seamless transition between manual mode and wire guidance mode, reducing any potential disturbances that may arise during the mode switch [4].

To mitigate disturbances when transitioning from manual mode to wire guidance mode, the control error, which serves as an input to the PI-controller, is set to zero when manual operation is active. As a result, an adjustment of the updating of the integral part in the PI controller occurs when manual operation is in effect, as defined in

$$I_k = I_{k-1} + K\frac{T_s}{T_i}e_k \tag{4.3}$$

$$I_k = I_{k-1} \tag{4.4}$$

Conversely, this adjustment does not affect the updating of the integral part when wire guidance mode is active, as specified in (4.3). By employing this adjustment, the integral part remains unchanged during manual operation, preventing any undesired updates during the mode switch and reducing the potential for a bumpy transition.

By implementing bumpless transfer, the control system ensures a seamless shift between manual mode and wire guidance mode, minimizing disturbances and providing a smoother and more reliable operation during the mode switch.

To achieve a smoother transition between manual steering and wire guidance mode, a gradual switch can be introduced when transitioning from manual mode to wire guidance mode. This gradual switch ensures that the influence of the control signal from manual steering does not abruptly disappear but is instead gradually reduced. At the same time, the impact of the control signal from the wire guidance mode is gradually increased. This gradual transition is depicted in Fig. 4.7.

On the other hand, when switching from wire guidance mode to manual operation, the transition is instant, as shown in Fig. 4.7. This means that the control signal from wire guidance mode is immediately replaced by the control signal from manual steering.

The implementation of this gradual switch between manual mode and wire guidance mode facilitates a smoother and more seamless transition, minimizing any abrupt changes in the control signals. By gradually adjusting the impact of the control signals during the mode switch, the control system can ensure a more comfortable and stable transition between the two modes.

The MATLAB functions used for this implementation can be found in Appendix B, providing further details and insights into the specific programming aspects of this gradual switch.

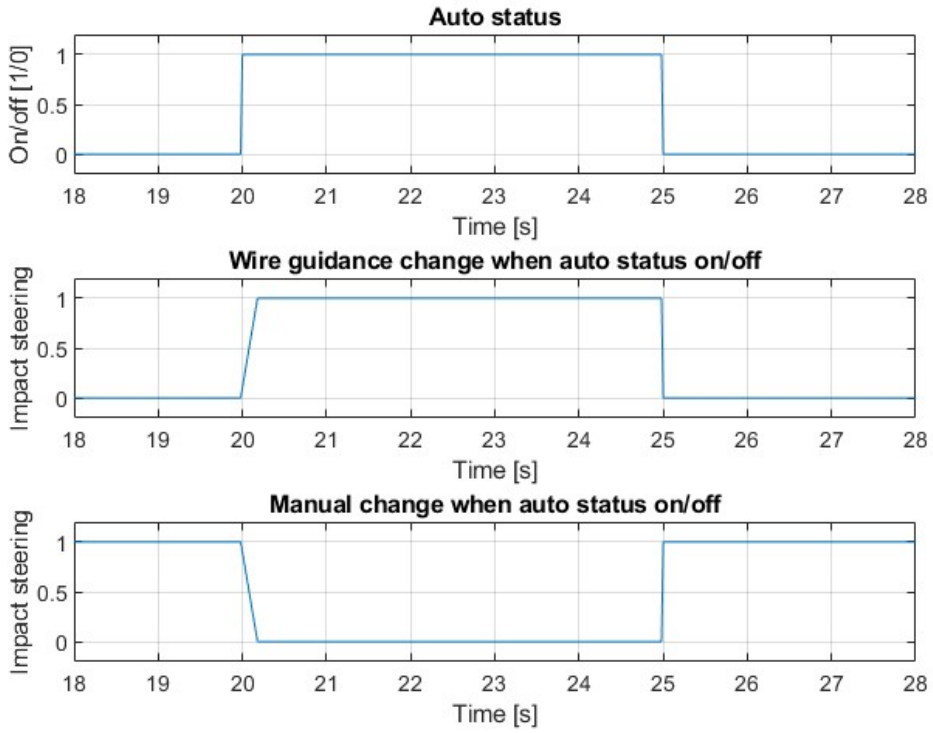

Figure 4.7: *How the impact of wire guidance steering and manual steering changes when auto-status is switched.*

4.4.5 Anti windup

The relationship between the valve position and the flow is generally linear until the valve reaches its fully open position. However, when the valve is fully open, it becomes saturated, which can lead to an undesirable wind-up effect in the integral component of the PI controller. This wind-up occurs because the controller continues to accumulate error in the integrator, even though the valve cannot respond to higher control signals beyond its maximum capacity.

The reason for this wind-up is the limited opening range of the valve, which prevents it from physically adjusting to higher control signals. As a result, the integrator component of the controller keeps accumulating error, leading to a degraded performance.

To address this issue, an anti-windup method called clamping is employed. Clamping aims to prevent the integrator from accumulating excessive error beyond the point of valve saturation. It does so by imposing a limit or *clamp* on the integral component, effectively stopping it from accumulating further error when the valve is fully open and unable to respond.

The clamping method ensures that the controller output never exceeds the saturation of the steering-command by imposing its own saturation limit (Fig.4.8). The values before and after the controller saturation are compared. If they are not equal, it indicates that the output has reached its saturation point, and further increase is prevented by saturating the output.

Additionally, if the controller output and input have the same sign, it signifies that the integral part is attempting to exceed the saturation zone, contributing to wind-up. In such cases, the solution is to send an error of 0 to the integral part. This effectively prevents the

accumulation of excessive error in the integrator, avoiding wind-up and maintaining stability in the control system [16].

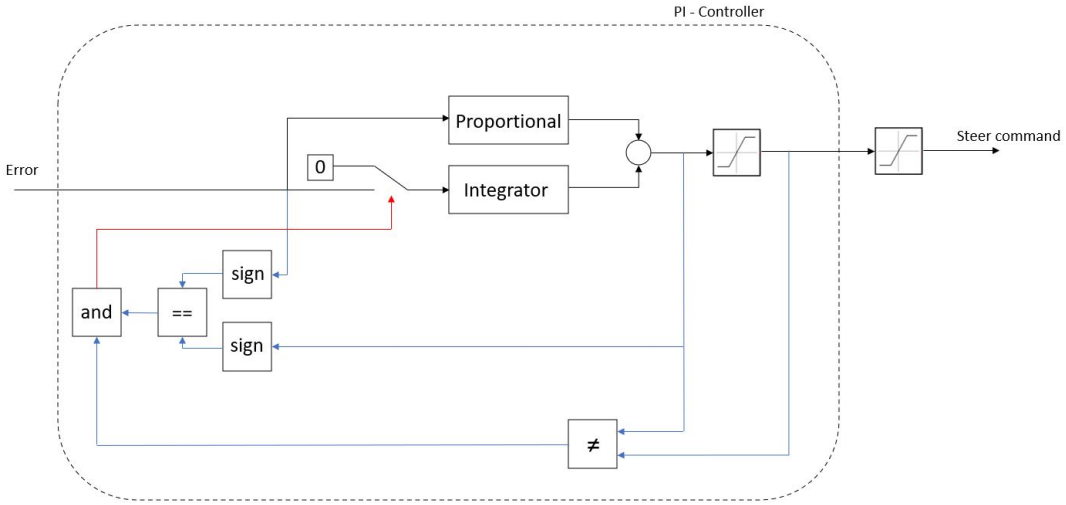

Figure 4.8: *Illustration of how the anti-windup works in the PI controller*

4.4.6 Methods for PI controller tuning

To obtain initial parameter values for the PI controller that controls the pivot angle, various tuning methods can be employed. One commonly used approach is the ad hoc method, where the controller parameters are set based on the user's knowledge and experience. This method involves manually adjusting the proportional and integral gains until the desired control performance is achieved.

Another approach is the model-based method, which utilizes a mathematical model of the system to determine the appropriate PI parameters. In the reference [6], several model-based tuning methods are proposed, including IMC (Internal Model Control) tuning, lambda tuning, and the Ziegler-Nichols method. These methods involve analyzing the system model and its response characteristics to select suitable values for the proportional and integral gains.

The PI controller in these tuning methods is typically represented in the Laplace domain using Laplace transforms, as described by

$$F(s) = K(1 + \frac{1}{T_i s}) \tag{4.5}$$

The model used for IMC and lambda tuning is

$$G(s) = \frac{K_p}{sT + 1} e^{-sL} \tag{4.6}$$

The system's static gain (K_p), time constant (T), and time delay (L) can be obtained through a step response experiment. However, in our case where the output is saturated and it is not possible to determine the system's static gain, the lambda and IMC tuning methods are not suitable options for setting the PI controller parameters. However, the Ziegler-Nichols method can still be applied using a different model representation, as described in

$$G(s) = \frac{b}{s} e^{-sL} \tag{4.7}$$

To apply the Ziegler-Nichols method, certain parameters in the model need to be determined through a step response experiment. The parameter b represents the steepest slope in the step response, and L represents the time delay. These parameters can be obtained for the system under consideration, allowing the use of the Ziegler-Nichols method to set initial values for the PI controller parameters.

According to the Ziegler-Nichols method, the initial values for the PI controller parameters are determined as $K = 0.9/(bL)$ and $T_i = 3L$. These initial values provide a starting point for the controller tuning process.

However, it is important to note that after setting the PI parameters using the Ziegler-Nichols method, further tuning is typically required to achieve the desired control performance. In this case, the ad hoc method can be employed to fine-tune the PI parameters based on the user's knowledge and experience. The ad hoc method allows for manual adjustments of the proportional and integral gains to optimize the control performance.

It is worth mentioning that the Ziegler-Nichols method is specifically used for setting initial values of the PI controller parameters controlling the pivot angle, while the ad hoc method can be used for tuning the parameters of the other controllers in the system. By combining the Ziegler-Nichols method for initial parameter estimation and the ad hoc method for further fine-tuning, a comprehensive approach to PI controller tuning can be applied to achieve the desired control performance in the system.

5 Results

In this chapter results from the modeling, manual steering and wire guidance steering are presented. It begins by showcasing the accuracy of the model and elucidating the disparities between the modeling and the real-world system. Furthermore, it evaluates the performance of manual steering and provides an explanation for the observed differences through the execution of multiple tests. Similarly, it investigates the performance of wire guidance steering and offers an explanation for the disparities through the implementation of various tests. The primary focus of these tests is the evaluation of locking times and smoothness.

5.1 Model

Fig.5.1 shows a comparison between the pivot angle obtained from simulation and the pivot angle measured through experimentation, using the same input signal. The results of the validation demonstrate a close approximation between the simulated and measured data. However, it should be noted that the model incorporates certain simplifying assumptions, which may introduce imperfections into the simulation. The accuracy of the model fit is quantified using the NRMSE, calculated using (3.1) and (3.2), which yields a value of 93.78%. This indicates a relatively high level of agreement between the simulated and measured data, considering the limitations and assumptions of the model.

Fig.5.2 depicts the simulated flow towards one of the cylinders when a ramp input is applied to the valve. The input signal to the valve gradually ramps from fully closed to fully open over a duration of 10 seconds. The plot demonstrates that in the model, there is a linear relationship between the valve opening and the flow of hydraulic fluid. This indicates that the pressure compensating valve is functioning as intended in the simulation.

However, at around 7.5 seconds, a drop in flow can be observed. This drop occurs because the piston reaches the top end of its stroke, resulting in an impact with the end-stop. The force generated by this impact causes a momentary displacement of the piston in the opposite direction. Nonetheless, due to the presence of pressure, the piston quickly returns to its initial position, resulting in a repetitive oscillatory motion after each collision with the top end, which is expected.

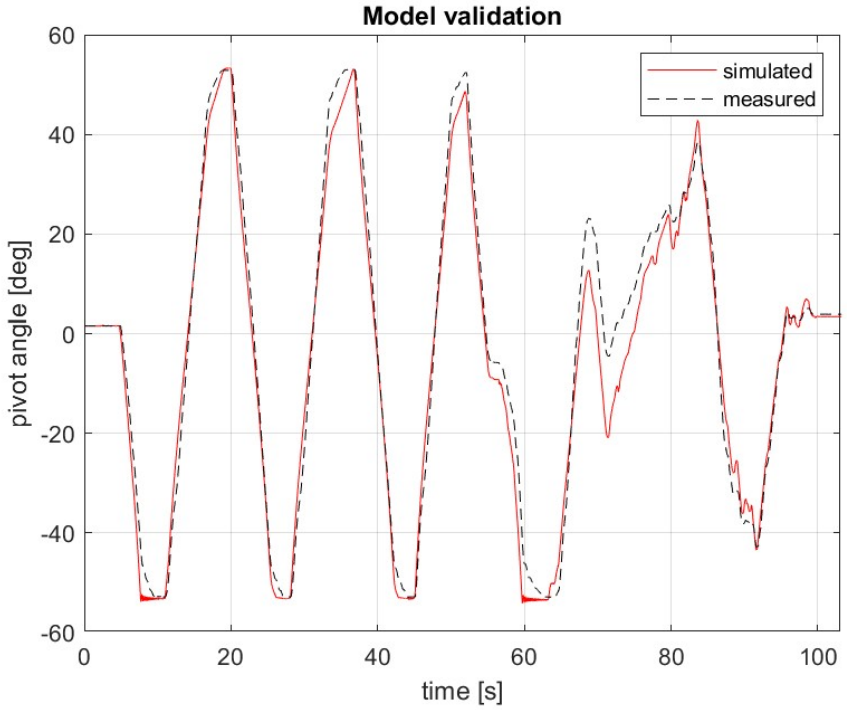

Figure 5.1: *The measured pivot angle vs the simulated pivot angle using the simulation model.*

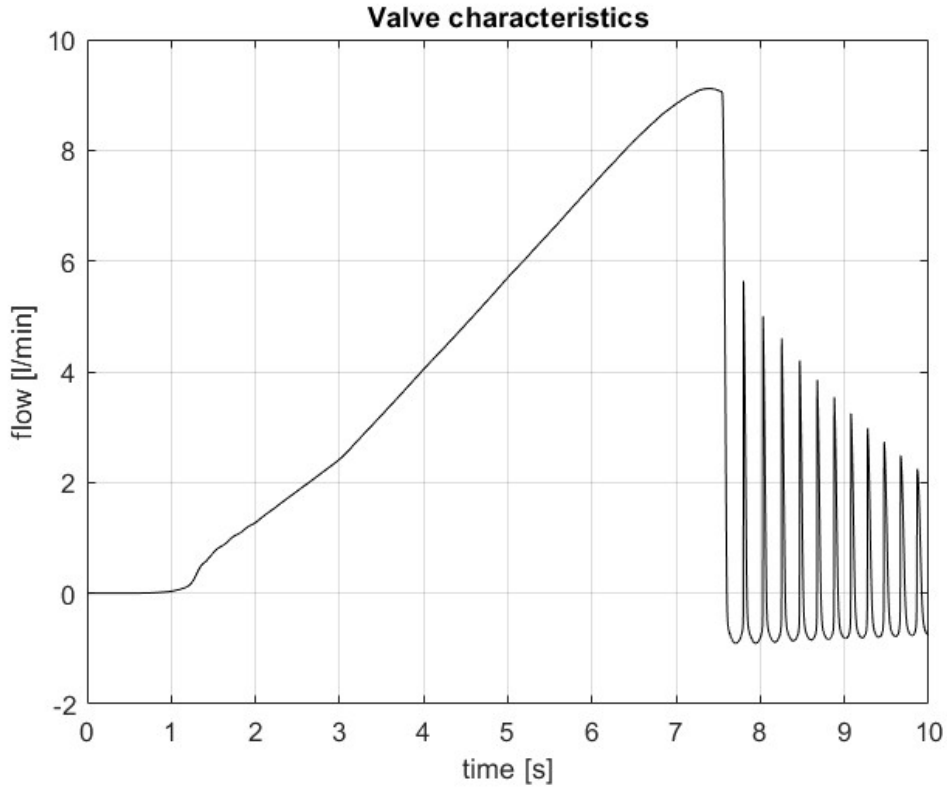

Figure 5.2: *The simulated flow from the valve for a ramp input.*

5.2 Manual steering

To assess the performance of manual steering, several tests were conducted. The first test involved applying maximum steering wheel input from one end position to the other, with the aim of evaluating the function of the soft stop mechanism at the two extremes. The speed of movement between the end positions was also measured for comparison.

The second test aimed to simulate fine adjustment of the forklift, which involved making rapid changes in the steering wheel input (as shown in Fig.5.4). This test was conducted to evaluate the smoothness of the steering system and compare it to the desired level.

The third test focused on a start-stop maneuver, where the input was stepped from zero to the maximum value and then back to zero (as illustrated in Fig.5.6). The objective of this test was to assess the delays and smoothness of the steering system during these transitions.

These tests provided valuable insights into the performance of the manual steering system, allowing for comparisons between different scenarios and helping to identify areas for improvement.

5.2.1 Test 1: Max turning

Fig.5.3 provides valuable insights into the performance of the forklift's steering system. Firstly, it demonstrates that the maximum pivot angle achievable by the forklift is approximately 52 degrees. Additionally, it presents a comparison of the changes in pivot angles between the end positions when the maximum steer speed input is applied. This comparison is made between the present configuration and the Speedgoat configuration.

The results show that the Speedgoat configuration outperforms the present configuration in terms of speed and efficiency. The time required to complete a full pivot from the maximum angle on one side to the other is approximately 6 seconds for the Speedgoat configuration, while it takes about 7 seconds for the present configuration. The two configurations decrease the time derivative of the pivot angle when it approaches its end position. However, the rate of decrease is slower in the current configuration compared to the Speedgoat configuration. This suggests that the Speedgoat configuration enables faster and more efficient steering in the end positions.

It is important to note that the observed time differences, particularly visible between time 10-11 seconds in Fig.5.3, are primarily due to the fact that the tests were conducted separately and under different conditions. Nonetheless, the results highlight the advantages of implementing the Speedgoat configuration in terms of improved speed, and efficiency during steering maneuvers.

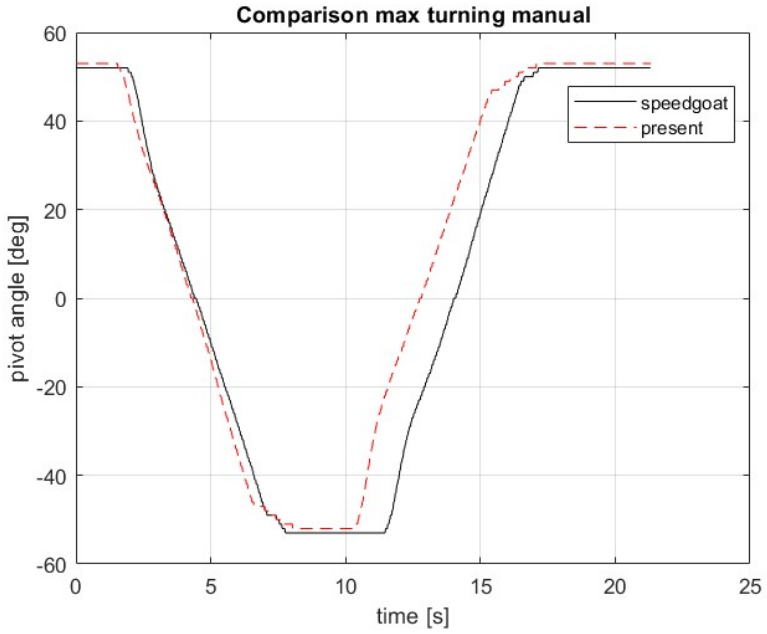

Figure 5.3: *Comparing the behavior and the differences in pivot angle (between the end positions) between the configurations when maximum steering speed is utilized.*

5.2.2 Test 2: Fine adjustment

Fig.5.4 and 5.5 provide a comprehensive comparison between the present configuration and the Speedgoat configuration in terms of their fast adjustment behavior. In Fig.5.4, the comparison is based on the response of the steering speed when rapid changes in steer wheel input are applied. These tests exhibit considerable similarity, thereby enabling a comparison of the currents between the configurations.

Fig.5.5 focuses on the change in current during the fast adjustment process. The change in current is more consistent and uniform in the Speedgoat configuration, indicating a more predictable and smooth steering at the expense of responsiveness when initiating the steering.

These findings demonstrate the advantages and the disadvantages of the Speedgoat configuration. It achieves smoother and a more predictable behaviour at the expense of the responsiveness when initiating the steering.

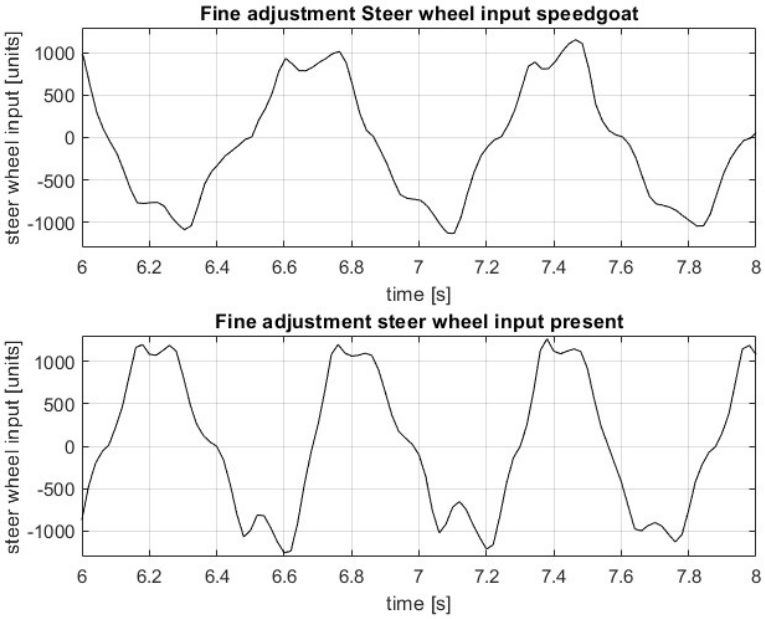

Figure 5.4: *The steering speed input for the manual configuration when doing fast changes on the steering wheel. Note the timescale.*

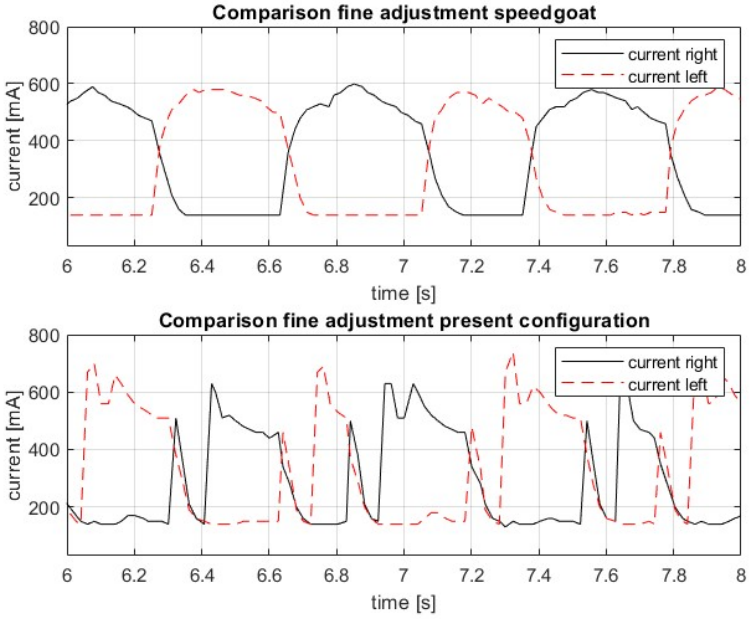

Figure 5.5: *The currents to right and left valves for the manual configuration when doing fast changes on the steering wheel. The input is Fig. 5.4.*

5.2.3 Test 3: Start and stop

Fig.5.7 and 5.6 present a comparison between the present configuration and the Speedgoat configuration to assess the start and stop behavior of the steering system. In Fig.5.7, the change in pivot angle is plotted over time for both configurations. By examining the corresponding steer wheel inputs in Fig. 5.6, the time delays for the start and stop behavior are calculated and summarized in Table 5.1.

The start delay refers to the time it takes for the pivot angle to change after the steering wheel sends a signal. It represents the response time of the steering system. The stop delay, on the other hand, is the time it takes for the pivot angle to stop changing after the steering wheel stops sending a signal. It indicates the system's ability to quickly and accurately halt the steering movement.

The values in Table 5.1 provide a clear comparison between the two configurations. These results indicate that the present configuration is more responsive, both when starting and when stopping.

Table 5.1: *The time delay when starting and stopping from first steering movement until the first change in pivot angle occurs.*

Controller	Start delay [s]	Stop delay [s]
Present	0.21	0.36
Speedgoat	0.31	0.54

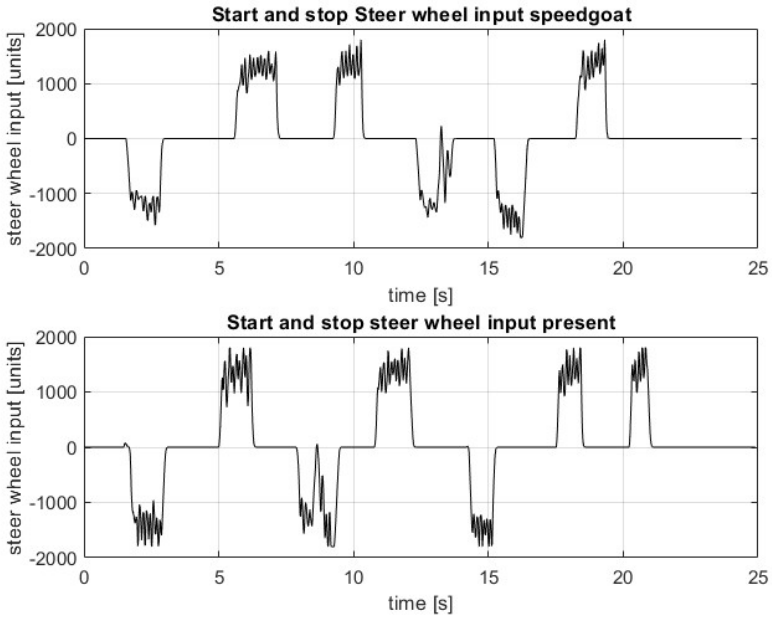

Figure 5.6: *The steering speed input for the manual configurations when the start and stop behaviour is evaluated.*

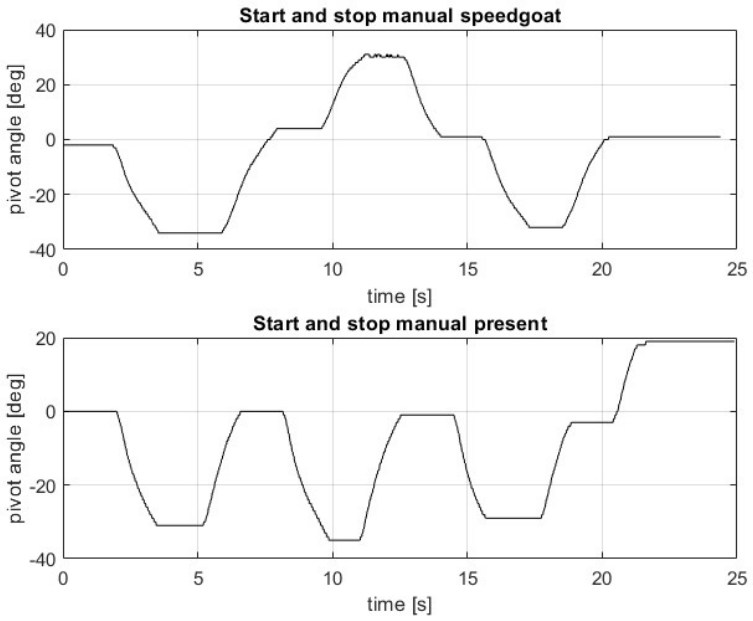

.

Figure 5.7: *The pivot angle changes for the manual configurations when the start and stop behaviour is evaluated. The input is shown in Fig.5.6*

5.3 Wire guidance steering

All tests are conducted when the forklift switches from manual to wire guidance mode. The timing of all tests is adjusted based on the activation of auto-status to ensure consistency. The primary objective of all tests is to maintain a high level of objectivity. In tests where active steering (i.e. the operator actively tries to acquire the wire manually) is not utilized, the starting positions, pivot angle and HA are kept as consistent as possible. When active steering is involved in the test, the steering aspires to be as similar as possible to make the results reliable.

The first test involved driving the forklift forward in its upright position at the maximum allowed speed (approximately 2.2 m/s) without any manual steering input. The angle of attack relative to the wire was nearly identical for both the present and Speedgoat configurations.

Similarly, in the second test, the forklift was driven in reverse without manual steering input. This test aimed to evaluate the performance of the steering systems in a different driving direction.

In the third test, a u-turn maneuver was performed before approaching the wire. This test aimed to simulate the typical driving behavior of an operator when navigating between two adjacent aisles. It was observed that the operator attempted to acquire the wire using active steering.

In the fourth test, the wire was acquired from the side with active steering aiming to replicate real-life scenarios where operators actively steer to acquire the wire. The speed during wire acquisition was approximately 2.2 m/s.

In the fifth test, the forklift acquired the wire at a slower speed of 1 m/s. This test aimed to simulate common situations where reduced speed is used when entering an aisle until the forklift is relatively upright. Active steering was also employed in this test to replicate

real-world conditions.

By conducting these tests under various driving conditions and scenarios, the performance of the steering systems in different situations can be assessed and compared between the present and Speedgoat configurations.

5.3.1 Test 1: Forward driving with no active steering

Fig.5.8 illustrates a comparison of HA, DFW, and pivot angle for the present configuration and the Speedgoat configuration. The initial values of HA and DFW, after wire detection, are similar between the experiments, indicating comparable starting conditions.

Initially, it can be observed that DFW exhibits slightly more oscillations for the present configuration. Furthermore, the present configuration shows more frequent switches between the valves, resulting in a bumpier behavior, particularly when the forklift is locked onto the wire (as depicted in Fig.5.9). In contrast, the Speedgoat configuration demonstrates a smoother operation, with HA and DFW stabilizing around 21.9 seconds, compared to 22.4 seconds for the present configuration (as shown in Fig.5.8).

The pivot angle in the Speedgoat configuration initially deviates slightly more, but it reaches a settling value faster compared to the present configuration. Moreover, the Speedgoat configuration requires fewer turns to reach the settling value (2 compared to 3), resulting in a smoother operation. The impact of the bumpless transfer is evident in Fig. 5.9, where the current gradually increases when the auto-status becomes active for the Speedgoat configuration, in contrast to the instantaneous increment observed in the present configuration.

In terms of wire locking time, both the Speedgoat and present configurations exhibit similar performance in this test, with a slightly faster locking time for the present configuration (as indicated in Table 5.2).

Table 5.2: *Time from auto-status is activated until the forklift is locked on the wire (Test 1)*

Controller	time until locked on wire [s]
Present	5.10
Speedgoat	5.22

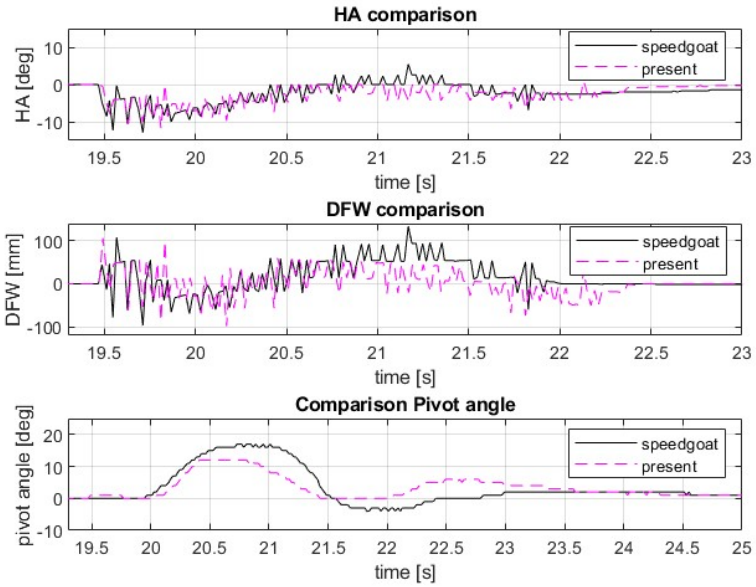

Figure 5.8: *The heading angle, distance from wire and pivot angle when starting with a nonzero angle and doing no active steering until the forklift is locked on the wire.*

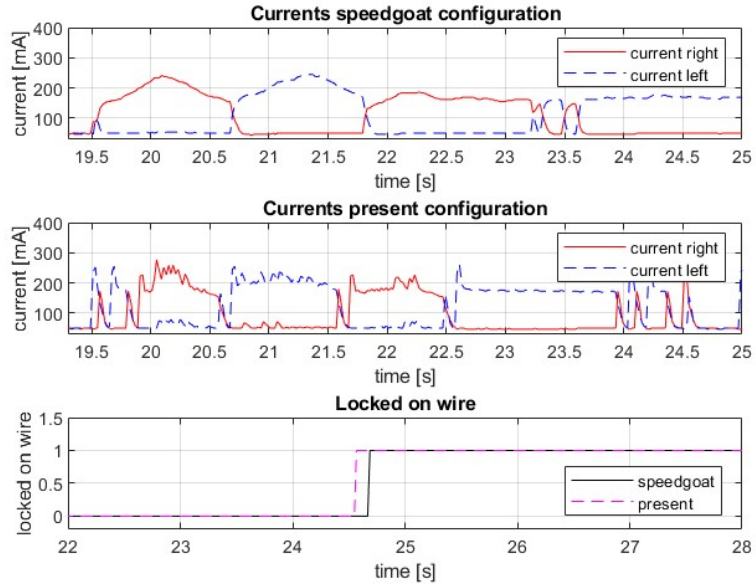

Figure 5.9: *The currents to the right and left valves when starting with a nonzero angle and doing no active steering until the forklift is locked on the wire.*

5.3.2 Test 2: Reverse driving with no active steering

Fig.5.10 presents a comparison of HA, DFW, and pivot angle for the present configuration and the Speedgoat configuration during reverse driving. It is evident from the analysis of the initial values after wire detection that the experimental conditions show a relatively similar nature in both configurations.

Throughout the experiment, the values for DFW and HA remain relatively similar between the present configuration and the Speedgoat configuration. However, the pivot angle for the present configuration deviates for a longer duration compared to the Speedgoat configuration. As a result, the Speedgoat configuration achieves faster wire locking (as indicated in Table 5.3).

Furthermore, the present configuration exhibits frequent switches between opening the left and right valves, particularly when the forklift is locked onto the wire. In contrast, the Speedgoat configuration demonstrates fewer switches, resulting in a smoother and less bumpy behavior (as shown in Fig. 5.11).

Table 5.3: *Time from auto-status is activated until the forklift is locked on the wire (Test 2).*

Controller	time until locked on wire [s]
Present	5.89
Speedgoat	4.25

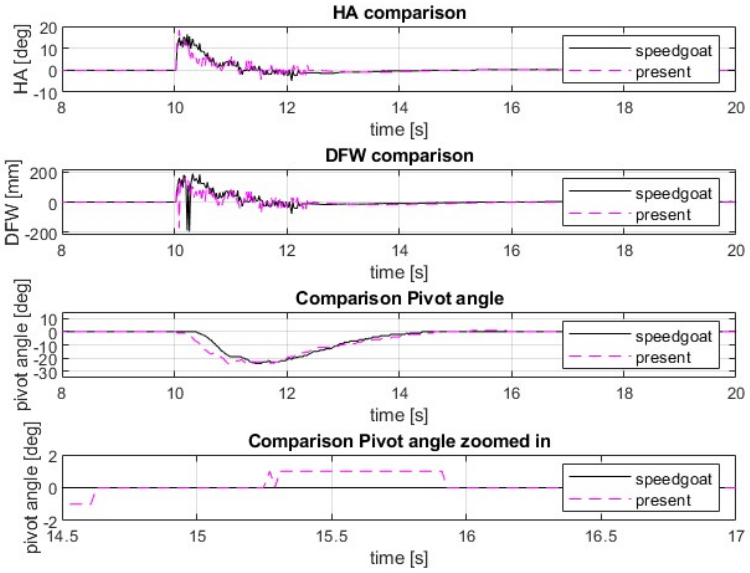

Figure 5.10: *Reverse driving. The heading angle, distance from wire and pivot angle when starting with a nonzero angle and doing no active steering until the forklift is locked on the wire.*

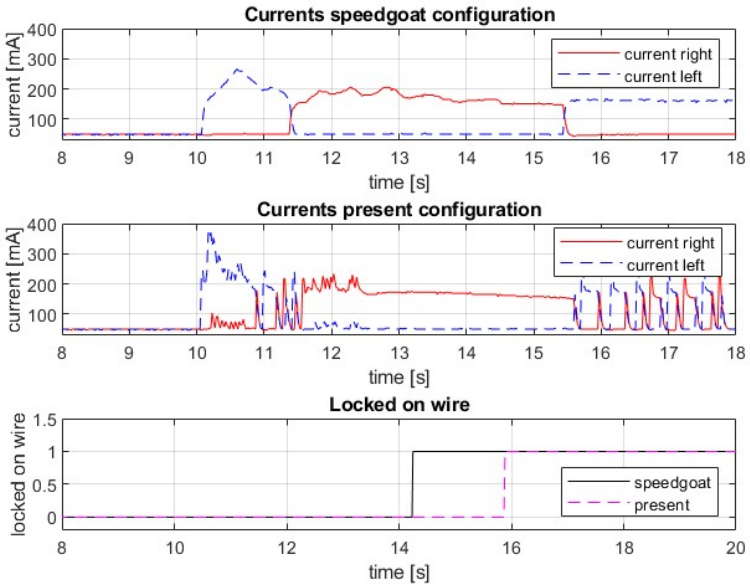

Figure 5.11: *Reverse driving. The currents to the right and left valves when starting with a nonzero angle and doing no active steering until the forklift is locked on the wire.*

5.3.3 Test 3: U-turn before acquiring wire

Fig.5.12 illustrates a comparison of HA, DFW, and pivot angle for the present configuration and the Speedgoat configuration during a u-turn maneuver. Observing the initial values following wire detection, it is apparent that the experimental conditions exhibit a substantial degree of similarity between the two configurations.

This particular test is more aggressive compared to the previous tests, resulting in larger values for HA and DFW when auto-status is activated (which occurs after approximately 10 seconds in Fig.5.12). In this case, the present configuration locks slightly faster to the wire (as shown in Table 5.4).

Initially, after auto-status is activated, both configurations exhibit significant oscillations in DFW and HA. However, approximately one second after activating auto-status (between 11 and 12 seconds in Fig.5.12), the Speedgoat configuration demonstrates smoother convergence towards zero for both DFW and HA. Furthermore, the present configuration, with frequent switches between the left and right valves, exhibits a more pronounced and bumpy behavior.

It is worth noting that in this test, the Speedgoat configuration shows a slight delay in response after auto-status is activated (approximately 0.2 seconds according to Fig. 5.12). Although this time difference varies slightly between different tests, the Speedgoat configuration generally exhibits a slightly slower reaction compared to the present controller.

Table 5.4: *Time from auto-status is activated until the forklift is locked on the wire (Test 3).*

Controller	time until locked on wire [s]
Present	8.85
Speedgoat	9.43

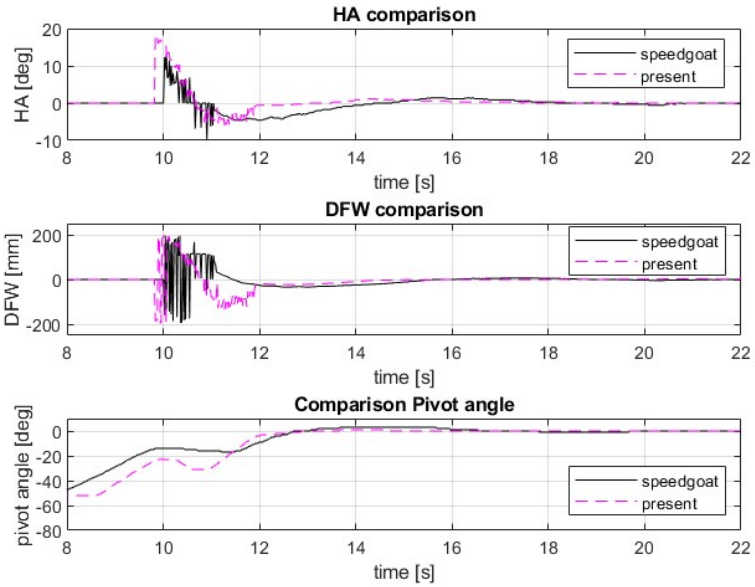

Figure 5.12: *The heading angle and distance from wire when doing a u-turn before acquiring the wire.*

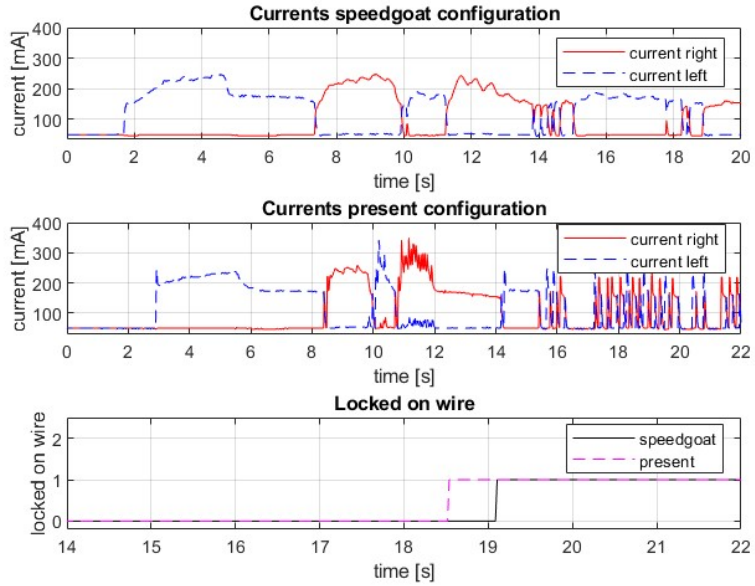

Figure 5.13: *The currents to the right and left valves when doing a u-turn before acquiring the wire.*

5.3.4 Test 4: Forward driving with active steering

Fig.5.14 presents a comparison of HA, DFW, and pivot angle between the present configuration and the Speedgoat configuration during forward motion with active steering. The analysis of the initial values subsequent to wire detection clearly indicates a notable resemblance in the experimental conditions between the two configurations.

Upon activating auto-status and when the forklift is locked on the wire, the present configuration exhibits quick switches between the valves, resulting in a bumpy behavior. In contrast, the Speedgoat configuration switches less frequently, leading to a smoother behavior (as depicted in Fig.5.15).

Despite the smoother behavior of the Speedgoat configuration, the present configuration demonstrates a slightly shorter locking time in this test (refer to Table 5.5). Although HA and DFW converge faster for the Speedgoat configuration, small deviations occurring between 16 and 20 seconds in Fig. 5.14 contribute to a longer locking time for Speedgoat.

Table 5.5: *Time from auto-status is activated until the forklift is locked on the wire (Test 4).*

Controller	time until locked on wire [s]
Present	9.03
Speedgoat	10.18

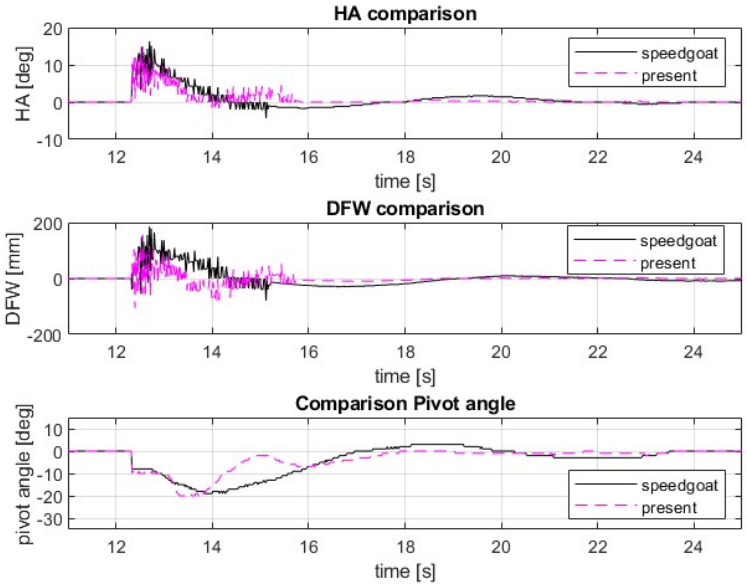

Figure 5.14: *The heading angle, distance from wire and pivot angle when the operator actively steers towards the wire.*

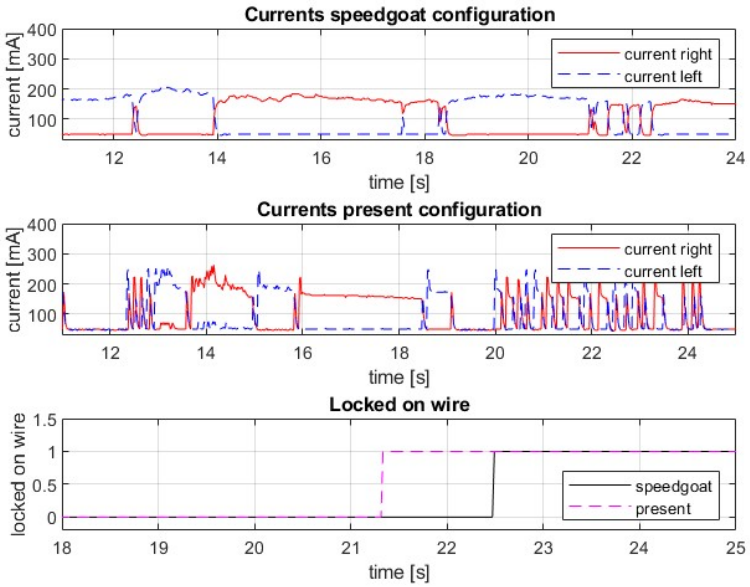

Figure 5.15: *The currents to the right and left valves when the operator actively steers towards the wire.*

5.3.5 Test 5: Slow driving with active steering

Fig.5.16 presents a comparison of HA, DFW, and pivot angle between the present configuration and the Speedgoat configuration during slow speed with active steering. Upon analyzing the initial values following wire detection, it becomes apparent that the experimental conditions are relatively comparable in both configurations.

In this test, the Speedgoat configuration demonstrates faster settling and less oscillatory behavior for HA, DFW, and the pivot angle. The Speedgoat configuration also achieves faster locking on the wire, as indicated in Table 5.6.

Moreover, the present configuration exhibits quick switches between the valves, particularly noticeable when the forklift is locked on the wire (as shown in Fig.5.17). This behavior results in a bumpy motion.

Table 5.6: *Time from auto-status is activated until the forklift is locked on the wire (Test 5).*

Controller	time until locked on wire [s]
Present	13.10
Speedgoat	12.41

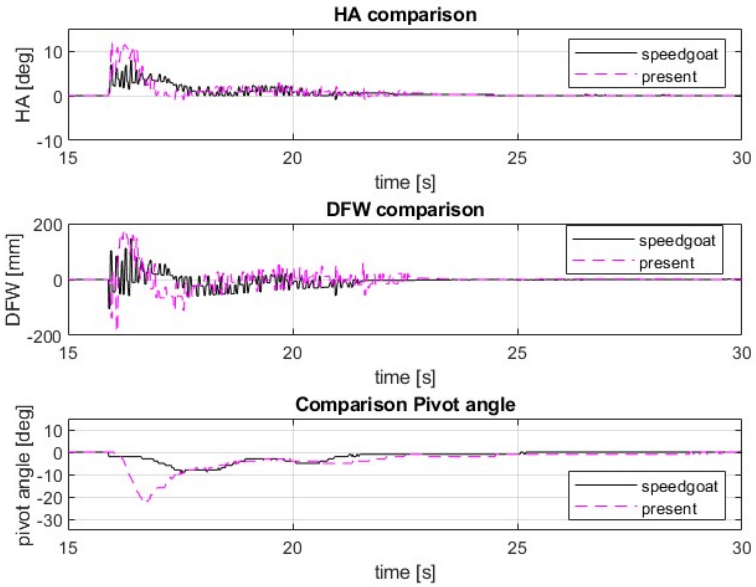

Figure 5.16: *The heading angle, distance from wire and pivot angle when the operator actively steers towards the wire and drives slowly.*

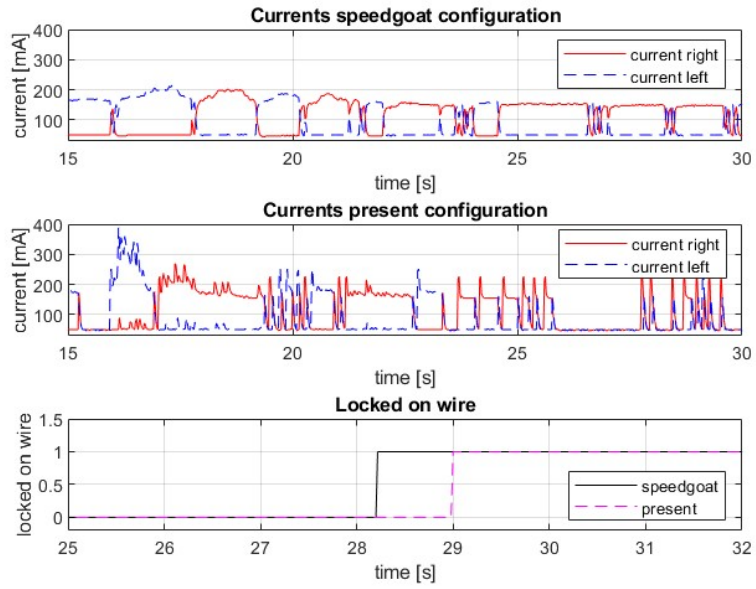

Figure 5.17: *The currents to the right and left valves when the operator actively steers towards the wire and drives slowly.*

6 Discussion

In this chapter the results from the modeling, manual steering and, wire guidance steering as well as ideas for future works are discussed.

6.1 Model

The model of the hydraulic and mechanical system of the steering function in the articulated forklift played a crucial role in designing the controller and evaluating its performance. Although achieving maximum accuracy in the model was desirable, its primary purpose was to assess the controller in simulation. Therefore, some simplifications and approximations were made to ensure a manageable modeling process, considering the complexity of the system with 164 different variables in Simscape.

The model for the manual configuration closely resembles the actual system, with a model fit of 93.78% according to NRMSE. Minor differences in the pivot angle can be observed when the cylinders approach the end position or during small fast adjustments (as shown in Fig.5.1). The model includes approximations for joint friction, cylinder leakage, and cylinder friction. While measuring these parameters would enhance the accuracy of the model, the approximations were deemed sufficient, and further improvements would likely have only a minor impact.

There were also uncertainties regarding certain other parameters in the model, particularly related to the pressure compensating valve. In the model, these parameters were approximated, but obtaining data from a datasheet or conducting more thorough investigations could lead to a more accurate model. Additionally, the model assumes a constant pressure source of 170 bar, while the actual forklift utilizes an hydraulic accumulator with a pressure ranging from 130 to 210 bar. Modeling the actual pump would improve the accuracy of the model, but this was considered a sufficient simplification given the expected time-consuming nature of developing a pump model. The difference caused by this simplification is minor and does not significantly affect the model fit.

In conclusion, while a more precise model could be achieved with additional time and effort, the current model is deemed suitable for its purpose. Further refinements would likely

result in only marginal improvements in accuracy, and the model adequately serves its role in evaluating and developing the manual controller.

6.2 Manual steering

In manual steering, there exists a trade-off between fast response time and smooth opening and closing of the valve. The Speedgoat configuration prioritizes a smooth operation of the valve, which results in a slower response time compared to the present configuration. The choice between a smoother operation or a faster response time depends on the preferences of the operator, as it is highly individual.

The Speedgoat configuration allows for faster steering when the pivot angle approaches its end position, as depicted in Fig.5.3. This faster steering can enhance productivity without causing a hard stop sensation for the operator. However, before implementing this configuration widely, it is important to conduct a detailed investigation into the potential wear on the cylinders resulting from the increased speed. Understanding the long-term effects and ensuring the durability of the system is crucial.

By carefully evaluating the wear and considering the preferences and needs of the operators, a decision can be made regarding the implementation of the Speedgoat configuration to increase productivity while maintaining satisfactory performance and longevity of the hydraulic system.

6.3 Wire guidance steering

The Speedgoat configuration demonstrates better handling in various driving scenarios compared to the present configuration. It exhibits less oscillatory and bumpy behavior, particularly when the forklift is approaching or locked on the wire. This improved behavior can be attributed to the Speedgoat controller's utilization of a derivative component on the HA, which reduces oscillations and overshoots. In contrast, the present controller employs a more aggressive control strategy with larger proportional gains, resulting in a jerky behavior with oscillations.

When the forklift is near the wire and locked on the wire, the current is limited, and the present controller's aggressive control strategy leads to frequent switching between the valves. This constant switching causes additional bumpiness in these stages, which becomes especially noticeable when physically standing on the forklift and comparing the two configurations.

Despite the more aggressive control strategy of the present configuration, the Speedgoat controller can compete in terms of locking time by using a variable P controller on the DFW. When DFW and HA are close to meeting the requirements for wire acquisition, the proportional part of the P controller is increased. This results in a greater steer command, leading to faster steering and a shorter time until the forklift is locked on the wire. Thus, the Speedgoat controller can achieve a comparable locking time while maintaining a smoother behavior during wire acquisition.

When driving at slower speeds, the controller has more time to steer back to the wire, improving the likelihood of wire acquisition without losing detection. In this scenario, smoothness becomes more important than higher steering commands. However, even though the present configuration sends lower steering commands at lower speeds, it still switches between the valves more frequently, resulting in a bumpy motion, which is perceived even more prominently at slower speeds.

In aggressive driving scenarios with larger angles of attack and higher speeds, the present configuration performs slightly better due to its more aggressive control strategy. It utilizes higher steering commands to acquire the wire at the expense of smoother steering. The Speedgoat configuration generally requires lower steering commands because the first 50% of valve opening corresponds to only 10% of the current and the proportional gains are smaller. However, when the angle of attack is large or when the operator is not actively trying to acquire the wire, larger steering commands are necessary. In such cases, the present configuration has a higher probability of wire acquisition due to its utilization of higher steering commands, albeit at the expense of smoothness.

Additionally, it is worth noting that there is a small time delay between the activation of auto-status and the first steering command in the Speedgoat configuration. This delay occurs because the signals controlling the steering are transmitted from the MCU to Speedgoat, processed through the controller to calculate the input currents, and then sent back to the MCU for steering control. Although this delay is small, it can affect the ability of the Speedgoat configuration to acquire the wire in aggressive driving scenarios. Implementing the controller in C code could eliminate this delay, but it would be time-consuming for this project, and the delay is generally insignificant.

The implementation of bumpless transfer, which reduces the impact of the wire guidance controller while switching between manual and wire guidance modes, also results in a reduced steering command initially. This reduction occurs over a 0.2-second period, during which the manual control signal is gradually diminished. Although this reduction has a relatively small impact, it limits the possibilities for wire acquisition during that period. However, the benefits of having a smooth transition outweigh the minor reduction in impact from the wire guidance controller. Bumpless transfer significantly reduces the bumpiness observed during mode switching, as seen in the currents in for example Fig.5.11. Moreover, aggressive driving on the wire is rare, making it more important to prioritize reducing bumpiness.

6.4 Future work

The behaviour of the forklift can still be improved. Here are some ideas that can be investigated in the future.

6.4.1 Exchange the proportional valve with a servo valve

Switching from a proportional valve to a servo valve in the forklift's steering system could indeed offer several advantages. Servo valves are known for providing more accurate control of flow and pressure, faster response times, and higher reliability compared to proportional valves [19]. These characteristics would likely result in a more precise and responsive steering control.

The faster response time of a servo valve would enable it to react quickly to changes in steering commands, improving the overall dynamic performance of the system. This could lead to smoother transitions between different steering modes, including the critical transition between manual and wire guidance mode.

However, it is important to consider the cost factor associated with servo valves. They tend to be more expensive compared to proportional valves, which could impact the feasibility of retrofitting the existing forklift with a servo valve. A cost-benefit analysis would be necessary to evaluate whether the expected improvements in steering performance justify the investment in a servo valve.

It is worth noting that while a servo valve could potentially enhance the forklift's steering system, it might not directly address the major problem of transitioning between manual and wire guidance mode. This issue is more complex and likely requires a comprehensive analysis and design approach to optimize the control strategy, sensor integration, and mode switching algorithms.

Further investigation and experimentation specifically focused on the impact of a servo valve on the forklift's steering performance, including its effect on mode transitions, could be a valuable area of exploration for future projects.

6.4.2 Model based control strategies

By devoting additional time to developing a comprehensive model for the the wire guidance mode, it becomes possible to explore model-based control strategies such as LQ, MPC, and feedforward control using a reference signal. One approach to creating the model is to utilize Simscape, extending the existing manual model to encompass the specific dynamics and behavior of wire guidance mode. Alternatively, MATLAB's system identification toolbox offers another option by estimating a model based on measured input and output data [15].

6.4.3 Reinforcement learning

Applying reinforcement learning in the wire guidance mode offers potential benefits. By considering relevant variables like DFW, HA, and pivot angle, reward functions can be defined for the agent. This approach holds promise for enhancing the system's performance. However, it remains uncertain whether it can effectively address the challenges associated with transitioning between manual and wire guidance modes. Further investigation is needed to determine the efficacy of reinforcement learning in solving this specific problem.

6.4.4 Redesigned hydraulic system

The improvement of steering in the hydraulic system is explored in [14], suggesting potential changes. One proposal is to expand the placement of the steering cylinders, which would increase the required flow and enhance steering controllability. Another suggestion involves redesigning the hydraulic system to incorporate two separate valves, each dedicated to a specific mode. In this design, the valve responsible for manual steering would be larger, while the valve for wire-guidance mode would be smaller. However, it is important to consider that implementing these suggestions would necessitate a time-consuming and costly redesign of the hydraulic system.

6.4.5 Iterative feedback tuning

Iterative Feedback Tuning (IFT) could be considered as a potential method to tune the PI controller responsible for sending out the steering-command. However, due to the unique nature of the control system, this would not be a typical IFT problem. The challenge arises when attempting to determine the derivative of the output signal, which is necessary for implementing IFT [11]. Further research and dedicated effort would be required to fully explore the potential benefits of IFT in this context.

6.5 Conclusion

The Speedgoat controller exhibits smoother behavior compared to the present controller, without causing any delay in wire acquisition. However, the Speedgoat configuration may face challenges when trying to acquire the wire in an aggressive manner. While exploring the potential benefits of a new hydraulic system to mitigate the zig-zag motion would be interesting, this thesis demonstrates that such behavior can be effectively suppressed by simply updating the controller.

7 Appendix

7.1 A

In this section, figures from the modelling are included.

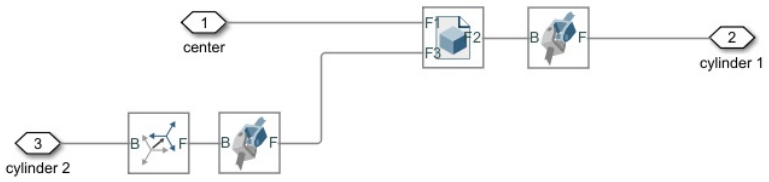

Figure 7.1: *A figure showing an example of how the parts are connected to each other using joints. This figure shows how the cylinders are connected to the rear part.*

7.2 B

In this section Matlab functions for bumpless transfer are included.

Ramping_up_control_signal_for_wire_guidance_steering.m

```
function angle_speed  = fcn(steer_cmd, auto_status,ramp_constant)

persistent gain_auto;
if isempty(gain_auto)
    gain_auto=0;
end

if auto_status==0
    gain_auto=0;

else
    gain_auto=gain_auto+ramp_constant;
    if gain_auto>=1
        gain_auto=1;
    end
end

angle_speed=gain_auto*steer_cmd;
```

Ramping_down_control_signal_for_manual_steering.m

```
function angle_speed  = fcn(ramp_constant,auto_status,SWU_angle_speed)
persistent gain_man;

if isempty(gain_man)
    gain_man=1;
end


if auto_status==0
    gain_man=1;

else
    gain_man=gain_man-ramp_constant;
    if gain_man<=0
        gain_man=0;
    end
end

angle_speed=gain_man*SWU_angle_speed;
```

Bibliography

[1] Karl Johan Åström and Tore Hägglund. *Advanced PID control*. Vol. 461. The Instrumentation, Systems, and Automation Society Research Triangle Park, 2006.

[2] Henrik Bäckman and Anders Brändström. *Modelling and Control of an Electro-Hydraulic Forklift*. Master's thesis, Linköping University, 2016.

[3] Erik Bodin and Henric Davidsson. *Model-Based Design of a Fork Control System in Very Narrow Aisle Forklifts*. Master's thesis, Linköping University, 2017.

[4] ControlSoft. *What's all the fuss about Bumpless Transfer?* Controlsoft, 2022.

[5] Csselectronics. *CAN Bus Explained - A Simple Intro [2023]*. URL: `https://www.csselectronics.com/pages/can-bus-simple-intro-tutorial` (visited on 05/15/2023).

[6] Martin Enqvist, Torkel Glad, Svante Gunnarsson, Peter Lindskog, Lennart Ljung, Johan Löfberg, Tomas McKelvey, Anders Stenman, and Jan-Erik Strömberg. *Industriell reglerteknik kurskompendium*. Reglerteknik, institutionen för systemteknik, Linköpings Universitet, 2014.

[7] Daniel Fahlén and Ludvig Fri. *Modelling and control of a forklift's hydraulic lowering function*. Master's thesis, Linköping University, 2017.

[8] *Formula book for hydraulics and pneumatics*. Linköping University, 2022.

[9] Torkel Glad and Lennart Ljung. *Reglerteknik: grundläggande teori*. Studentlitteratur AB, 1981.

[10] Torkel Glad and Lennart Ljung. *Reglerteori: flervariabla och olinjära metoder*. Studentlitteratur, 2003.

[11] Håkan Hjalmarsson, Svante Gunnarsson, and Michel Gevers. *Model-free tuning of a robust regulator for a flexible transmission system*. Elsevier, 1995.

[12] Lovisa Jansson and Amanda Nilsson. *Evaluation of Model-Based Design Using Rapid Control Prototyping on Forklifts*. Master's thesis, Linköping University, 2019.

[13] Zhizheng Jiang and Benxian Xiao. "LQR optimal control research for four-wheel steering forklift based-on state feedback". In: *Journal of Mechanical Science and Technology* 32 (2018), pp. 2789–2801.

[14] Emil Johansson. *Simulation and evaluation of an articulated forklift truck*. Master's thesis, Linköping University, 2014.

[15] Lennart Ljung. *System identification toolbox: User's guide*. Citeseer, 1995.

[16] Mathworks. *Anti-windup for PID control | Understanding PID Control, Part 2*. 2018. URL: https://se.mathworks.com/videos/understanding-pid-control-part-2-expanding-beyond-a-simple-integral-1528310418260.html (visited on 05/09/2023).

[17] Olof Olsson and Karl-Erik Rydberg. *Kompendium i hydraulik*. Linköping University, Institute of Technology, 1993.

[18] Rolf Roskam. "Development of a Forklift for Research and Education in Mechatronics". In: *Proceedings of the 2018 2nd International Conference on Mechatronics Systems and Control Engineering*. 2018, pp. 17–21.

[19] Karl-Erik Rydberg. *Hydraulic servo systems: dynamic properties and control*. Linköping University Electronic Press, 2016.

[20] Tua Agustinus Tamba, Bonghee Hong, and Keum-Shik Hong. "A path following control of an unmanned autonomous forklift". In: *International Journal of Control, Automation and Systems* 7.1 (2009), pp. 113–122.